

Old Dominion University

ODU Digital Commons

Electrical & Computer Engineering Theses &
Dissertations

Electrical & Computer Engineering

Spring 2003

Adaptive Segmentation Techniques for Object Region Extraction from Images with Complex Lighting Environment

Deepthi P. Valaparla
Old Dominion University

Follow this and additional works at: https://digitalcommons.odu.edu/ece_etds



Part of the [Electrical and Computer Engineering Commons](#)

Recommended Citation

Valaparla, Deepthi P.. "Adaptive Segmentation Techniques for Object Region Extraction from Images with Complex Lighting Environment" (2003). Master of Science (MS), Thesis, Electrical & Computer Engineering, Old Dominion University, DOI: 10.25777/a0nw-m947
https://digitalcommons.odu.edu/ece_etds/548

This Thesis is brought to you for free and open access by the Electrical & Computer Engineering at ODU Digital Commons. It has been accepted for inclusion in Electrical & Computer Engineering Theses & Dissertations by an authorized administrator of ODU Digital Commons. For more information, please contact digitalcommons@odu.edu.

**ADAPTIVE SEGMENTATION TECHNIQUES
FOR OBJECT REGION EXTRACTION FROM IMAGES
WITH COMPLEX LIGHTING ENVIRONMENT**

by

Deepthi P Valaparla
B. Tech. June 2000, Jawaharlal Nehru Technological University

A Thesis Submitted to the Faculty of
Old Dominion University in Partial Fulfillment of the
Requirement for the Degree of

MASTER OF SCIENCE

ELECTRICAL ENGINEERING

OLD DOMINION UNIVERSITY
May 2003

Approved by:

Vijayan K. Asari (Director)

Stephen A. Zahorian (Member)

W. Steven Gray (Member)

ABSTRACT

ADAPTIVE SEGMENTATION TECHNIQUES FOR OBJECT REGION EXTRACTION FROM IMAGES WITH COMPLEX LIGHTING ENVIRONMENT

Deepthi P Valaparla
Old Dominion University, 2003
Director: Dr. Vijayan K. Asari

Automated image segmentation of objects in complex lighting environments is a difficult task since it is not possible to pre-define a threshold to distinguish the object from the background. It is ascertained that an effective threshold criterion for such objects depends on the negative binomial distribution of the object region with respect to the background lighting. Based on this concept, a novel adaptive threshold selection method for automatic segmentation of the lumen region in endoscopic images is presented in this thesis. More precise lumen region and boundary are obtained by an integrated neighborhood search based region growing procedure whose speed is significantly enhanced by a quad-tree structure decomposition method. A boundary thinning and connecting algorithm, employing a novel search window on the preliminary boundary, provides a single-pixel-width-connected boundary. The new method does not need *a priori* knowledge about the image characteristics and is completely automatic. It reduces the computation time by 36% when compared to conventional threshold selection methods and facilitates high-speed response for real-time navigation of a vision-guided micro robotic endoscope.

A new adaptive threshold selection method for skin extraction from the normalized r-g histogram of a face image is also presented in this thesis. It is observed from the spatial analysis of the r-g histogram that skin regions appear as clusters having negative binomial distribution characteristics, thus enabling accurate skin extraction from

the background which is random or uniform. The textures of the candidate skin region are further analyzed using wavelet packet decomposition to obtain a set of feature vectors. Classification of the regions as face or non-face is done by evaluating the Bhattacharya distance of each feature vector to a prototype vector. The adaptive method has an improved accuracy of 9% when compared to traditional face detection techniques with images in varying lighting conditions. Research is progressing towards development of a relative variance based lighting compensation technique to segment static color images in normalized color space.

Copyright, 2003, by Deepthi P Valaparla. All Rights Reserved

This thesis is dedicated to
The GOD almighty,
my family for their love,
my advisor Dr. Vijayan K. Asari for his support ,
and my friends who have stood beside me.

TABLE OF CONTENTS

LIST OF TABLES.....	viii
LIST OF FIGURES.....	ix
CHAPTER	
1. INTRODUCTION.....	1
1. 1. Adaptive Segmentation.....	1
1. 2. Automatic Threshold Selection.....	2
1. 3. Methodology.....	3
1. 3. 1. Lumen thresholding.....	3
1. 3. 2. Lumen boundary extraction.....	4
1. 3. 3. Skin thresholding.....	4
1. 3. 4. Wavelet analysis.....	5
1. 3. 5. Shape analysis.....	5
1. 4. Results.....	5
1. 5. Summary.....	7
2. REVIEW OF EXISTING TECHNIQUES AND ALGORITHMS.....	8
2. 1. Adaptive Segmentation.....	8
2. 2. Advances in Adaptive Segmentation.....	9
2. 2. 1 Biology and Biomedical imaging.....	9
2. 2. 2. Biometrics.....	9
2. 2. 3. Document analysis.....	10
2. 2. 4. Adult supervision issues.....	10
2. 3. Techniques in Adaptive Segmentation	11
2. 3. 1. Histogram thresholding.....	11
2. 3. 2. Edge detection.....	12
2. 3. 3. RG histogram thresholding.....	13
2. 3. 4. Wavelet analysis.....	14
2. 4. Summary.....	15
3. PROBLEM STATEMENT AND THEORETICAL DEVELOPMENTS.....	16
3. 1. Adaptive Segmentation for Lumen Region Extraction.....	16
3. 1. 1 Histogram-based thresholding techniques.....	17
3. 1. 1. 1. Otsu's method.....	17

3. 1. 1. 2. Recursive thresholding technique.....	19
3. 1. 1. 3. Adaptive progressive thresholding algorithm....	22
3. 1. 1. 4. Automated thresholding algorithm.....	23
3. 1. 2 Region extraction.....	26
3. 1. 2. 1. Pyramidal quad tree strucures.....	26
3. 1. 2. 2. Integrated neighborhood search.....	28
3. 1. 2. 3. Back-projection algorithm.....	29
3. 1. 3 Obtaining the lumen boundary.....	30
3. 1. 3. 1. Boundary extraction.....	30
3. 1. 3. 2. Boundary thinning.....	31
3. 1. 3. 3. Boundary linking.....	32
3. 2. Adaptive Segmentation in Face Detection.....	33
3. 2. 1. Histogram-based thresholding techniques.....	34
3. 2. 1. 1. Waibel et al.'s method.....	34
3. 2. 1. 2. Adaptive skin thresholding technique.....	36
3. 2. 2. Face detection	37
3. 2. 2. 1. Wavelet analysis.....	38
3. 2. 2. 2. Form factor analysis	40
3. 2. 2. 3. Morphological operation.....	41
3. 3. Summary.....	43
4. SIMULATION RESULTS	44
4. 1. Lumen Region Extraction with Adaptive Thresholding Algorithm.....	44
4. 2. Adaptive Segmentation for Face Detection.....	49
4. 3. Summary	54
5. CONCLUSION.....	55
REFERENCES.....	57
CURRICULUM VITAE.....	63

LIST OF TABLES

Table	Page
4. 1. Experimental results showing difference in processing time between APT and ATA based methods.....	51
4.2. Table for 256*256 images comparing percentage success rate for the conventional algorithm and the proposed method.....	56

LIST OF FIGURES

Figure	Page
1.1. Endoscopic test image and its extracted lumen region.....	6
1.2. Test image and its face detection results using adaptive skin thresholding.....	6
3.1. Original gray-scale image and its gray scale histogram.....	17
3.2. Image thresholded by the Otsu method and its histogram.....	18
3.3. Original document image and its histogram.....	20
3.4. Document image after the first recursive iteration and its histogram.....	20
3.5. Document image thresholded completely to obtain only the text regions.....	21
3.6. Endoscopic image thresholded with Cheriet's method.....	21
3.7. Endoscopic image thresholding using the adaptive thresholding algorithm (APT)...	22
3.8. Flow diagram of the adaptive thresholding algorithm.....	25
3.9. Image thresholded with the adaptive thresholding algorithm.....	25
3.10. Hierarchy of levels in a pyramidal quad tree structure.....	27
3.11. Illustration of the back-projection algorithm.....	29
3.12. Boundary extraction preferential sequence search window.....	31
3.13. Boundary thinning illustration.....	32
3.14. Boundary linking illustration.....	33
3.15. A training image and its r-g histogram.....	35
3.16. Conventional skin segmentation with universal thresholds on sample image I.....	35
3.17. Conventional skin segmentation with universal thresholds on sample image II.....	35
3.18. Sample image III thresholded with adaptive skin thresholding technique.....	37
3.19. Wavelet decomposition into detail and approximation images shown at 3 levels...	39
3.20. Sample Image III after wavelet analysis.....	41

3.21. Sample Image III after form factor analysis.....	41
3.22. Candidate face regions back-projected and thresholded using the ATA technique.....	42
3.23. Morphological operation on the ATA threshold candidate face regions.....	42
4.1. Endoscopic image thresholded using ATA.....	45
4.2. Daughter images generated using the quad structures.....	45
4.3. Integrated neighborhood search result for the daughter image.....	46
4.4. Back-projection from a daughter image onto the parent image.....	46
4.5. Edge-detected parent image.....	47
4.6. Thinning algorithm application and binarization.....	47
4.7. Thinning result of sample image I with final boundary extracted.....	48
4.8. Original sample image II with extracted lumen boundary.....	48
4.9. Original sample image III with extracted lumen boundary.....	48
4.10. Sample image I for face detection routine.....	50
4.11. Result of adaptive skin threshold method.....	50
4.12. Result of the wavelet analysis result of the grayscale image.....	51
4.13. Result of shape analysis using the form factor.....	51
4.14. Binarized version of image in Fig. 4.13.....	52
4.15. Sample image I and the final result showing faces bound with a box.....	52
4.16. Sample image II and final result.....	53
4.17. Sample image III and final result.....	53
4.18. Sample image III and final result, also shows two of the missed detections.....	53

CHAPTER 1

INTRODUCTION

Image processing in real-world applications has sought to apply human reasoning to computer programs for image segmentation. Numerous methods with unparalleled accuracy have been put forward to get to algorithms, which can effectively segment the object from the background. The applications broadly range from medical imaging, intruder detection, adult supervision on the Internet, to security issues in the working environment and public safety. This thesis is an attempt to address the problem of automated image segmentation, with a focus towards developing robust adaptive thresholding algorithms that can work without a predefined set of limiting parameters in complex lighting environments. The exercise has provided valuable insight into the designing, development and testing of a self-reliant and easy to use endoscopic lumen extraction method and a wavelet based face detection technique.

1. 1. Adaptive Segmentation

Most image-based computer applications require a good segmentation result for subsequent operations such as feature extraction, feature recognition, and object classification. An ideal segmentation algorithm would yield accurate results for a large and diverse set of test images. The difficulty is compounded when the system needs to adapt to changes in image quality, imaging devices, and varying lighting conditions. Non-adaptability of systems to varying intensities and devices produce poor segmentation results. Adaptive image segmentation extracts the object using the image statistics,

instead of relying on the trained parameters to achieve the optimal set of threshold constraints for segmentation. Probability distributions, such as the negative binomial distribution, can be used to model the object region statistically and extract the object with its relative variance measure.

1. 2. Automatic Threshold Selection

Thresholding has always been a forerunner for the image segmentation task due to its simplicity. Automated threshold selection in image segmentation is still a major challenge to researchers.

Gastrointestinal images are captured by CCD cameras embedded in an electronic endoscope. A light source at the tip of the endoscope illuminates the tract and helps the camera to capture the image at an instant. Regions closer to the camera are illuminated well and seem brighter. The region where the light intensity is the lowest and appears to be dark is called the lumen region and is the space through which the physician needs to maneuver the endoscope without causing any physical injury to the tract. Extraction of the lumen region from the thresholded image in an accurate and efficient manner facilitates accurate navigation of the endoscope. An automated threshold selection method using the image histogram in this process would greatly enhance the endoscope's ability since the lumen varies from person-to-person in age, size of the tract, and also background illumination conditions.

The ability to detect the location and region boundaries of a face in an image with varying color content and illumination characteristics can make the task of human recognition easier. Automatic threshold selection can be used for detection of faces in poorly lit images without having to train images for setting pre-defined face detection

thresholds. Histogram-based automatic threshold selection in the normalized color space provides excellent results for face images.

1. 3. Methodology

Conventional methods for the process of image segmentation are region-based (region growing and texture based segmentation) and edge-based (active contour models and dynamic programming approaches). It has been observed that statistical analysis of image data is needed for a good segmentation result. A comprehensive outline of histogram-based lumen thresholding, lumen boundary extraction, histogram-based skin thresholding, wavelet decomposition and shape analysis methods, which have aided in the segmentation task, are presented as methodology tools.

1. 3. 1. Lumen thresholding

A gray-scale version of the endoscopic image is used to compute a histogram of the image. An iterative process suggested by Otsu maximizes the normalized between-class variance of two classes of the histogram to find the threshold. The Adaptive Thresholding Algorithm (ATA) computes a progressive histogram containing the gray levels below the Otsu threshold, and uses the relative variance as a threshold selection criterion to decide if the correct amount of separability has been achieved between the object and the background. The process is recursive and takes very little time when compared to conventional threshold selection methods. It also provides the flexibility to work on any image, as it uses the immediate image statistics instead of pre-set parameters.

1. 3. 2. Lumen boundary extraction

A pyramidal quad-tree structure compresses the thresholded lumen region into a smaller size by creating daughter images, and thus minimizes the search area while saving valuable computation time. The lumen region's center of mass in the daughter image is used as a seed pixel to propagate in an eight-neighborhood search of the seed pixel to find the lumen region. In doing so, other unwanted regions outside of the lumen boundary region, which prop up during thresholding, are eliminated. A back-projection algorithm projects the lumen region pixels from the daughter image onto the original parent image. Boundary pixels of the extracted lumen region are found with a boundary search algorithm. A preferential sequence search, using a novel window for thinning, eliminates redundant pixels from the extracted lumen region boundary. The boundary pixels are then linked together to obtain a single-pixel-width-connected boundary.

1. 3. 3. Skin thresholding

Accurate skin extraction is needed for face region segmentation. The red and green components of the color image are normalized. A histogram of values, with frequency of the occurrence of the combinations of red and green intensities, at different pixel locations throughout the original image for 64 different 32×32 regions is plotted. The image's information is now stored within 4096 histogram locations of each of the 32×32 regions. The relative variance is computed for the red axis as DR and the green axis as DG for each of the 64 histograms. A threshold value having a combined occurrence of $0.5 \leq DR \leq 1$ and $0.4 \leq DG \leq 0.9$ is considered as being a skin region. All the gray levels corresponding to these combinations are back-projected onto the original image. Skin regions and non-skin regions with a similar texture are obtained as a result.

1. 3. 4. Wavelet analysis

Each of the thresholded regions is bound in a square box and a set of feature vectors are computed using wavelets. Skin regions have lesser deviation coefficient values as compared to non-skin regions. A threshold for the Bhattacharya distance from the feature vectors to a prototype vector eliminates non-skin regions similar to the skin.

1. 3. 5. Shape analysis

The form factor of each segmented skin region can lead to a face or non-face classification based on shape information. Since a face region is nearly circular or elliptical, it will have a form factor close to 1. Thresholding involves segmenting out non-face regions having a lesser form factor. The adaptive thresholding algorithm is used to threshold out dark regions in the resulting image. A rectangular operator widens these dark features like eyes, nose and eyebrows in the image. If the algorithm finds the required number of holes in a candidate region, it is identified as a face.

1. 4. Results

The image in Fig. 1 shows an image subject to the segmentation process and its result with the lumen boundary extracted. The lumen region boundary is a single-pixel-width-connected boundary. The extraction process is done in real-time and significant improvement in the high-speed response has been noted. The proposed skin thresholding and face detection technique yields good results, as is evident from the result of the test image in Fig. 1.2.

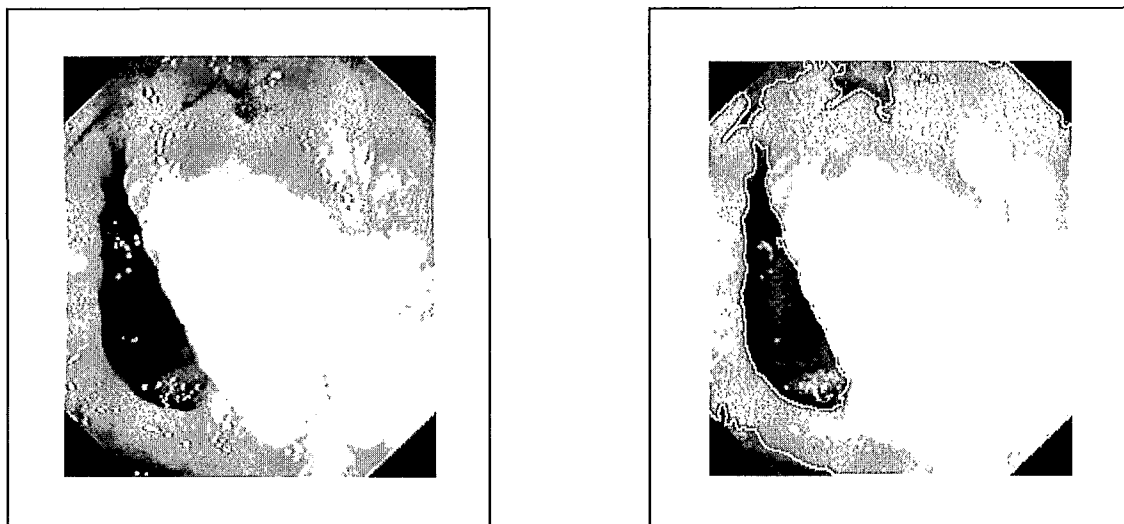


Fig.1.1: Endoscopic test image and its extracted lumen region.



Fig.1.2: Test image and its face detection results using adaptive skin thresholding.

Efforts are ongoing to modify the algorithm to segment CAT scan images and also to develop an algorithm for effective segmentation of document images. Progress is also being made in extracting face features with varying poses.

1. 5. Summary

Automated segmentation in complex lighting environments can be achieved by using statistical analysis of image histograms. Since object regions correspond to the negative binomial distribution, the relative variance measure can be used as a threshold selection criterion. The proposed adaptive thresholding algorithm incorporates the relative variance for an improved and faster segmentation result as compared to its predecessor. The ability to maneuver a micro-robot based endoscope is a real-time application and can be made more effective through the proposed method. Detecting the presence of faces in an image can be automated with the proposed dispersion factor based histogram technique.

An extensive literature survey has aided the progress to a large extent and is cited in the second chapter. The third chapter describes the crux of the thesis and gives insight into the development of an adaptive segmentation algorithm for endoscopic images. It also includes the design and implementation of a face detection algorithm, which is aided by a new histogram technique for effective skin separation and wavelets based face detection. Results of these experiments and illustrated applications arising from this research are presented in chapter four. The final chapter concludes the thesis with retrospection into the performance and suggestions on continuing this work.

CHAPTER 2

REVIEW OF PRESENT TECHNIQUES AND ALGORITHMS

Advances in science and research form the basis for development of cutting edge tools for the end-user. In the course of the experiments and trials conducted to aid this thesis, many published articles were researched and referred to. This is an endeavor to document the resources and research materials which have aided this thesis.

2. 1. Adaptive Segmentation

Image segmentation has always been a powerful tool for researchers in the creation of an effective separation mechanism. Recognizing homogeneous regions in an image as being distinct and labeling them as objects can be termed image segmentation. It is a preprocessing tool in object identification and plays an important role in image analysis. There are many issues that need to be addressed in this regard. A literature survey documented in [1] reviews the present techniques in image segmentation. More comprehensive reviews have been presented in [2, 3] to elucidate the existing trends in image segmentation.

While image segmentation researchers have focused their energies and resources to build robust algorithms for effective object extraction, some have tried to make the process more robust by incorporating the adaptivity aspect to the problem. The combination of an adaptive clustering algorithm with a simple texture segmentation approach is used for adaptive color image segmentation [4]. An adaptive approach to texture-feature segmentation for multi-channel wavelet frames and two-dimensional envelope detection for natural and synthetic textures has yielded excellent results [5].

2. 2. Advances in Adaptive Segmentation

Applications ranging from biomedical imaging, document analysis, biometrics, motion analysis to fault detection in industrial materials have set new trends in the scientific community. The need for automation and real-time analysis demands faster and more accurate technology. An exhaustive survey of these methods provides a better understanding into the handling and understanding of processed image data.

2. 2. 1. *Biology and Biomedical imaging*

An environmentally adaptive segmentation algorithm by [6], based on a partially supervised learning process, developed for outdoor field plant detection, had an accuracy increase of more than 54.3%. An efficient and adaptive multi-grid level set method for front propagation purposes in three dimensional medical image processing and segmentation, which deals with non sharp segment boundaries, is presented in [7].

The ability to maneuver a micro robotic endoscope through the intestinal tract, using a pneumatic system [8], requires deftness and diligence on the part of surgeons. An inch-worm like mechanism presented in [9] employs an air bellow for locomotion and vacuum devices for clamping. A smart colonoscope system proposed by [10] with special functions such as locomotion, auto-camera steering and human friendly interface also offers key technologies like virtual biopsy and advanced diagnosis. Biomedical imaging thus relies heavily on adaptive medical image segmentation for effective target region extraction.

2. 2. 2. *Biometrics*

Biometrics has gained respectability in areas of surveillance, face recognition, content-based retrieval, adult supervision on the Internet and intelligent systems. Face

identification using visible spectrum images have been used in [11] for human and machine identification of faces. A face detection method suggested in [12] constructs eye, mouth, and boundary maps for verifying each probable face candidate. Several patents have been registered in the development of face recognition systems for the purpose of video surveillance and security purposes.

2. 2. 3. Document analysis

Document image processing has become a big industry, owing to the popularity of printed documents as a medium of communication. The use of these aids in large numbers can be cited as the main reason for automated real-time document imaging and analysis systems. A text extraction technique proposed in [13] aims at segmenting text from shaded or textured backgrounds and non-structured layouts. Document image clean up and binarisation presented in [14] smoothens and enhances the textual content in an image. The frequency of the background texture is supposed to have a higher frequency. Threshold for text extraction is computed via the intensity histogram of the binarized image. Further applications include the optical character recognition systems which have helped in building more accurate and effective mechanized aids for reading and understanding documents.

2. 2. 4. Adult supervision issues

The availability of graphic content on web pages has grown into a significant problem with more people having easier access to the World Wide Web. While one can debate over self-imposing rules to help overcome this crisis, researchers have turned to machines for answers. It has helped to build systems like the one suggested in [15] by using skin

extraction and grouping to later analyze the skin content and filter obscene materials. Although legal statutes bind people under the law to desist from indulging in these activities, the success of computer software in regulating obscenity has made this growing field an active research topic.

2. 3. Techniques in Adaptive Image Segmentation

Adaptive image segmentation relies on various methods to extract objects from images. Techniques used for gray level images are histogram thresholding, quad tree structures and edge detection. Color images are segmented with the r-g histogram threshold selection method, wavelet analysis and morphological processing. A comprehensive summary of the reviewed articles is presented here.

2. 3. 1. Histogram thresholding

Thresholding is an important part of pre-processing of an image. It essentially separates the target image from the background with a fair degree of accuracy. A survey of thresholding techniques presented by Sahoo et al. [16], Lee et al. [17] and Wezska [18] summarizes the extent to which thresholding has been refined for use in image segmentation. The Otsu's method [19] is used as the basic idea for image thresholding. Based on variances derived from the probability theory, it maximizes the normalized between-class variance for divided classes in the histogram. The optimum threshold value corresponds to the gray level with the maximum normalized between-class variance. Cheriet's recursive thresholding [20] segments the Otsu image until no new peaks are found in the histogram or the region in question becomes too small. It has been known to work well with document images and bank checks, but is limited to images with only two

classes. The Adaptive Progressive Thresholding (APT) technique [21] uses the recursive Otsu method with a separability factor to decide when to stop its iterative computations.

The image has a spatial distribution that is random in nature. The measures of randomness suggested in [22, 23] provide a number of ways for the analysis of image characteristics. It is assumed in spatial data analysis that the observations follow a Poisson distribution. A natural test for the Poisson distribution is the relative variance measure suggested in [24, 25]. Adaptive thresholding algorithm (ATA) [26] has incorporated the relative variance factor into the APT and terminates the algorithm at the appropriate time with better results than the APT. The results produced by the ATA have far exceeded the expectations in terms of automation and much needed real-time processing capability.

2. 3. 2. Edge detection:

The camera at the end of the endoscope takes real-time pictures for the purpose of processing and intestinal lumen edge detection. Since thresholding alone cannot guarantee an exact boundary of the segmented image, further processing is needed to obtain a single-pixel-width-connected boundary. Some well researched edge detection techniques have been presented in [27]. A region analysis procedure in which similarities between neighboring pixels are examined is presented by [28]. A dual-step approach combining token matching and neighborhood search has been proposed in [29] for accurate extraction of the centers of the dots contained in a rectangular grid. A highly unpredictable structure of the endoscopic image makes it impossible for the use of this technique for intestinal lumen extraction.

A learning-based method has been suggested by [30] to enhance the reliability of

the segmented region. Region-splitting using a recursive method was suggested by [31] for segmenting color pictures. Pyramidal quad trees [32] have been used to minimize the area and increase the speed of reconnaissance in the thresholded image for lumen extraction and representation. This method extracts only an approximate lumen region in the form of a combination of several rectangular blocks of pixels. An integrated neighborhood search and back-projection as suggested by [33] is conducted to find the object region devoid of any unwanted regions. Segmented region growing in [34] combines the region growing and edge detection methods for segmenting the images. The method is iterative and uses both of these approaches in parallel. The algorithm starts with an initial seed located inside the true boundary of the region. The pixels that are adjacent to the region are iteratively merged with it if they satisfy a similarity criterion.

A knowledge-based process for thinning alphabet boundaries has been presented in [35] which is rather ineffective for thinning the lumen region boundary. The thinning process suggested in [26] uses a preferential sequence search with two windows to get a single-pixel width lumen boundary. A boundary connection algorithm suggested in [36], uses an intermediate pixel optimization scheme to ensure connectivity between adjacent boundary pixels. The result is a boundary through which the micro robot can navigate without causing any injury to the walls of the intestines.

2. 3. 3. RG histogram thresholding

Among the techniques for extracting objects in color images, r-g histogram thresholding is the most notable. It was suggested by [37] that distribution of color information can be used to localize objects in color images. One can deal with the inconsistency in observation of the surface reflection by searching for clusters of color in an image. In an

RGB histogram object clusters form streaks. Though the histogram technique includes the expensive time constraint, the adaptive aspect of the histograms was used by [38] for offline computation and database image retrieval.

Modeling of the target image after normalizing the three primary colors in two-dimensional chrominance space has been suggested by [39, 40, 41] to manipulate camera orientation and keep track of human faces at all times. A multimodal interface with neural networks for an online human face classifier and tracker is proposed in [42] to aid videoconferencing applications.

A system for locating the focus of attention of a person [43] using normalized r-g histograms yielded appreciable results and led to this technique being used to develop histograms with more advanced color detection algorithms. Facial feature extraction from color images presented in [44] proves that normalization reduces the difference of color distribution. A real-time face tracker proposed in [45] characterizes skin color distributions of human face, estimates image motion and compensates for camera motion while being used as a powerful tool in teleconferencing.

Diversifying a bit further into the field of face detection, one can say that normalized color distributions for different faces are less variant in normalized color space than in RGB color space. A new algorithm for histogram-based skin threshold selection that incorporates the relative variance [46, 47] of the region's frequency distribution is presented in this thesis.

2. 3. 4. Wavelet analysis

Wavelets are being widely used as a tool in image processing for frequency analysis based texture segmentation. The short-time or windowed Fourier transform and the

wavelet transform procedures are compared in [48] for an effect on the frequency analysis of a time-dependent signal. A signal decomposition technique that decomposes a signal into different frequency bands is studied in [49]. A two-step analysis is used in both frequency and time domain, to separate the spectral envelop from fine spectral details and to extract smooth temporal trajectory of the spectral envelopes. Successive decomposition of a continuous signal by a pair of low pass and high-pass filters to give the discrete wavelet transform was suggested by [50, 51].

With regards to this thesis, face detection using wavelets that have been used in [52] is very instrumental to classify regions as skin and non-skin for further processing. The concept of feature vector classification has been dwelt on to a large extent in [53]. Estimation of the proximity between two probability distributions presented in [54] was done by evaluating the Bhattacharya distance, rather than the divergence measure. The Bhattacharya distance measure has also been used in [55] for detection in Markov chains. A more comprehensive distance-measuring scheme proposed in [56] has significantly aided in thresholding regions having the same texture as the skin.

2. 4. Summary

The articles reviewed in this section have greatly influenced the progress of this thesis. While focusing on the broader perspective of writing algorithms for making better devices, this exercise has provided a valuable insight into the amazing methods and devices available in the real world.

CHAPTER 3

PROBLEM STATEMENT AND THEORETICAL DEVELOPMENTS

The goal of this thesis has been to develop segmentation algorithms, which are adaptive and aid real-time applications with improved speed and accuracy. This section broadly deals with the statement of the problems and the solutions proposed in this thesis.

The difficulty in extracting the intestinal lumen boundaries for navigating through the gastrointestinal tract is stated as the first problem. Reliable adaptive thresholding algorithms for faster and accurate boundary region extraction have been proposed as a solution to threshold the lumen region, and extract its boundaries. A feature detection exercise involving the detection of faces in complex lighting environments is stated as the second problem. An adaptive skin thresholding technique has been proposed as a solution to aid effective skin extraction. Texture and shape analysis help eliminate non-skin and non-face regions and thus aid in the face detection.

3.1 Adaptive Image Segmentation for Lumen Region Extraction

Region detection and extraction processes for many applications needs to be made adaptive, partly due to the fact that all images do not share the same characteristics and lighting conditions. The application of adaptive image segmentation to endoscopy involves the use of techniques such as gray-level thresholding, region detection and boundary extraction. The surgeon needs the precise boundaries of the lumen region for calculations that can lead to a correct diagnosis. An in-depth view of the present techniques and their drawbacks constitute the first part of this section, with the second section focusing on the proposed algorithm and its working.

3.1.1 Histogram Threshold selection techniques:

Threshold selection using histograms has always been the automatic choice for the image segmentation task. It provides the flexibility of experimenting with gray levels and also deals with the segmentation problem from a statistical standpoint.

Fig. 3.1 shows an image of the intestinal lumen as captured by an endoscopic camera. Since the histogram has many peaks, the problem of threshold selection becomes complicated. Existing techniques have proposed unsatisfactory ways of extracting the threshold. An adaptive thresholding method has been proposed and described at the end of this section to extract the lumen region boundaries in a faster manner.

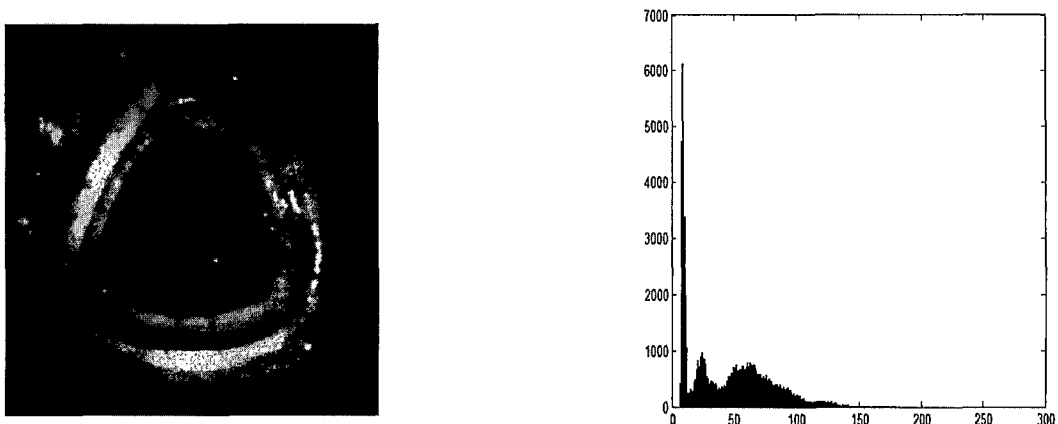


Fig. 3.1: Original gray-scale image and its gray scale histogram.

3.1.1.1 Otsu's method:

Based on the variances of the statistical properties of the image, the procedure begins by defining the global mean of the image [19]. The gray level histogram of the image is computed and divided into two classes. Cumulative moments of the zeroeth and the first

order of the histogram are computed to the i^{th} level. The total mean (μ_T) and the global variance (σ_T^2) are computed. An iterative computation is performed to the maximized normalized between-class variance (σ_B^2) which is defined as the weighted-variance of the cluster means themselves around the overall means. The gray-level with the maximum between-class variance is designated as the optimum threshold level.

The test image which has been thresholded, using the Otsu method, and its histogram with gray levels above the threshold eliminated are shown in Fig. 3.2.

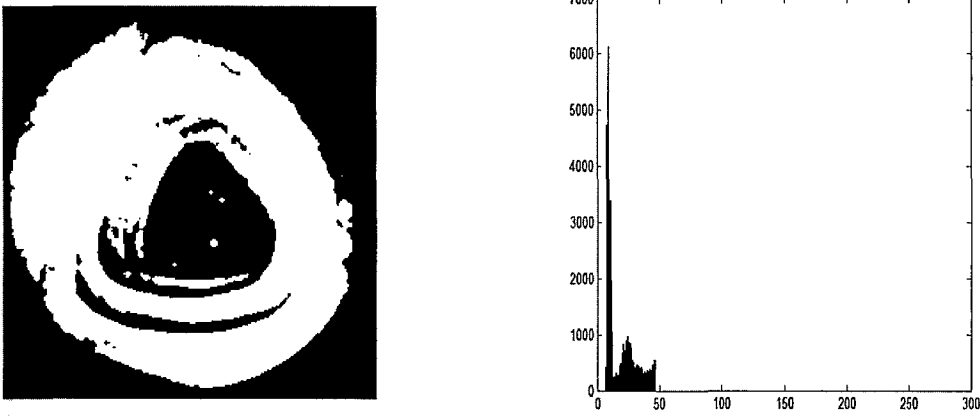


Fig. 3.2: Image thresholded by the Otsu method and its histogram.

Otsu's method evaluates the goodness of the threshold by using the discriminant analysis.

$$\sigma_B^2 + \sigma_W^2 = \sigma_T^2, \quad (3.1)$$

where σ_W^2 is the within-class variance. σ_B^2 is based on first-order statistics and σ_W^2 is based on second-order statistics. The total variance σ_T^2 is always constant for a given image. The maximized between class variance maximizes the distance between the object

and the background classes and gives an appreciable separability of the threshold but is not really appropriate for lumen region thresholding as is evident from Fig. 3.2.

3.1.1.2 Recursive Thresholding Technique [20]

Otsu's method is not suitable for all applications, as it can threshold only the high-intensity regions which are a result of the mucosal reflections in the image. The procedure devised by Cheriet *et. al* involves an iterative computation to compute the threshold value for an image. Otsu's method partitions an image into two classes and provides a good distinction between the classes. This property of Otsu's method is used to detect the optimum threshold t_1^* between the two classes.

The recursive thresholding algorithm works on the progressive histogram of the previously thresholded image. It computes a new histogram, which only has the intensities below t_1^* of the thresholded image. This process is continued until no new peaks in the histogram are encountered or the regions in question become too small. This technique is effective in segmenting the darker regions from the rest of the image as seen from the results of the document image. The first document image and its histogram are shown in the Fig. 3.3. After it is thresholded, using the Otsu's method, all the gray levels above the threshold value are discarded. A new histogram is computed from the thresholded gray levels. This process is continued iteratively until the separation factor between the means of the two classes is less than 90%. When the separation factor exceeds 90%, the iterations are stopped and the final result is the darkest region in the image as is evident from the results. The method only performs well on the images with two classes. Iteratively, it can be used to segment more than two objects in an image.

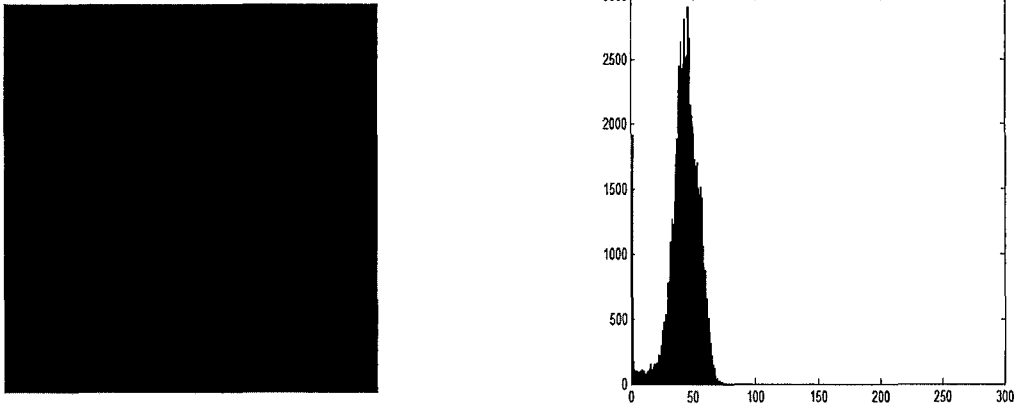


Fig. 3.3: Original document image and its histogram.

It was concluded that the algorithm gives good results when the target is the darkest object in a test image as is evident from Fig. 3.4 and Fig. 3.5. The lumen region has not been properly detected in the endoscopic image shown in Fig. 3.6, but apparently it shows the darkest region of the image.

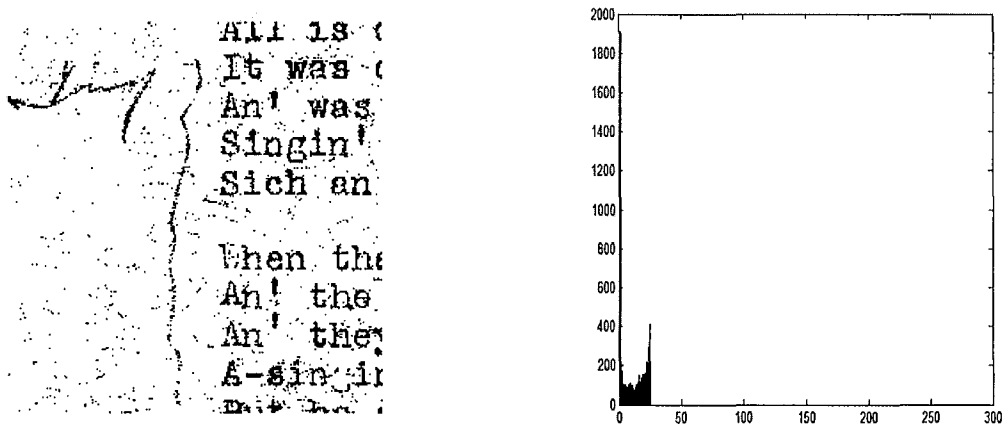


Fig. 3.4: Document image after the first recursive iteration and its histogram.

All is
It was
An' was
Singin'
Sich an

When the
An' the
An' they
A-singin'
But he

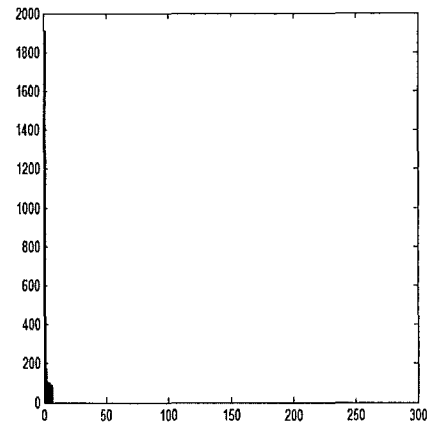


Fig. 3.5: Document image thresholded completely to obtain only the text regions.

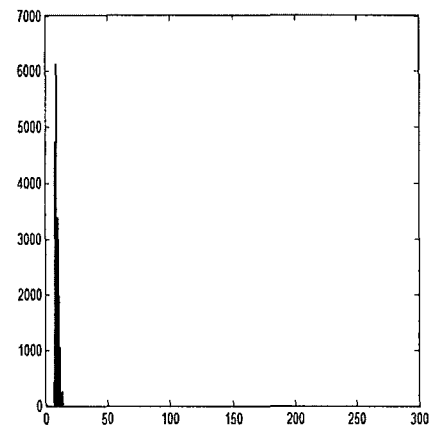


Fig. 3.6: Endoscopic image thresholded with recursive thresholding method.

It fails to provide a properly segmented image with complex background, such as our test image of Fig. 3.1, where the segmentation result should be the lumen region. The reason for failure of this method, when applied to an endoscopic image, can be attributed to choosing an incorrect separability factor.

3.1.1.2. Adaptive Progressive Thresholding Algorithm [21]

This algorithm makes use of both the Otsu's technique and the recursive method. It has a cumulative limiting factor, which is computed at the end of each recursive computation and is compared with a factor called as the separability factor. The cumulative limiting factor is defined as

$$\text{CLF}(\Delta) = \frac{\sigma_B^2(\Delta)}{\sigma_T^2} \text{ for } \Delta \geq 1 \quad (3.2)$$

The $\text{CLF}(\Delta)$ is calculated for each progressive image and compared with the separability factor. Thus the process stops when,

$$\text{CLF}(\Delta) < \alpha \frac{\mu_T}{\sigma_T^2} \quad (3.3)$$

This method employs α known as the limiting parameter, which can be trained using a number of images taken from a same camera. Results of APT are shown in Fig. 3.7.

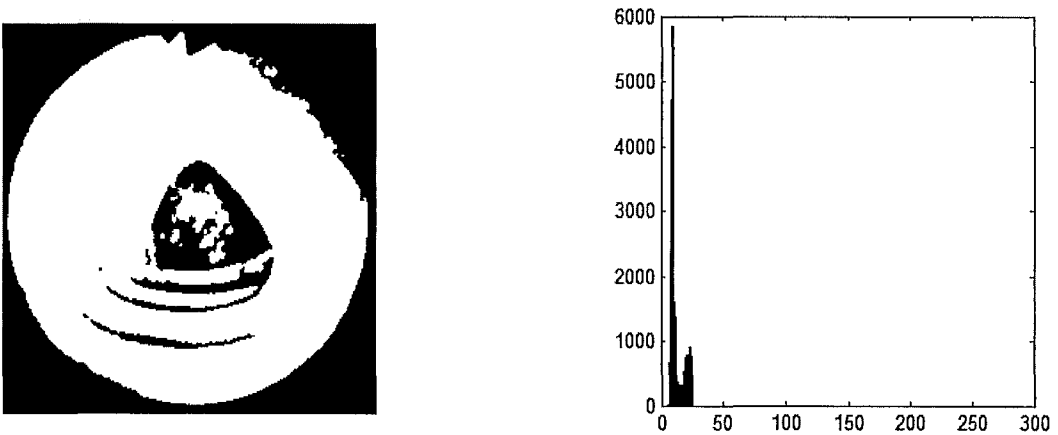


Fig. 3.7: Endoscopic image thresholding using adaptive thresholding algorithm (APT).

3.1.1.4 Automated Thresholding Algorithm [26]

The basic shortcoming of APT is that the value of α is a pre-defined factor, which is not derived from the parameters of the image. The value of α is different for images captured with different cameras. It also depends on the reflection characteristics of the object and the lighting environment of the image. Thus, APT falls short of providing a thresholding algorithm that is completely image-dependent and that uses the image parameters. It is not suitable for real-time applications because of the large number of iterations. The proposed technique is described as follows:

The image consists of L gray levels and has a size of $M \times N$ pixels. The spatial location of a pixel (x, y) corresponds to a gray level $g'(x, y)$. The image function as a mapping can be defined as

$$g : M \times N \rightarrow P \quad (3.4)$$

A smoothed image can be generated by passing the image through a smoothing filter S of size $s \times s$. The smoothed image is represented as

$$g'(x, y) = \frac{1}{s^2} \sum_{(k,l) \in S} g(x+k, y+l) \quad \forall (x, y) \in M \times N \quad (3.5)$$

The initial stage is based on Otsu's method. This partitions the L gray levels in the image into two classes, $P_0 = \{0, 1, 2 \dots t\}$ and $P_1 = \{t+1, t+2 \dots L-1\}$ at gray level t . The total variance (σ_T^2) and the between-class variance (σ_B^2) are computed. The normalized between-class variance ($\frac{\sigma_B^2}{\sigma_T^2}$) is maximized, and the optimum threshold t^* is the gray level corresponding to the maximum normalized between-class variance.

$$t^* = \text{Arg} \max_{0 \leq i < L} \left\{ \frac{\sigma_B^2}{\sigma_T^2} \right\} \quad (3.6)$$

$$\sigma_B^2 = \left(\sum_{i=0}^t \frac{n_i}{N} \right) \left(1 - \sum_{i=0}^t \frac{n_i}{N} \right) (\mu_1 - \mu_0)^2 \quad (3.7)$$

$$\sigma_T^2 = \sum_{i=0}^{L-1} (i - \mu_T)^2 \frac{n_i}{N}, \quad (3.8)$$

where

$$\mu_T = \sum_{i=0}^{L-1} \frac{in_i}{N} \quad (3.9)$$

is the total mean of the original image, N is the total number of pixels present in the image, n_i is the number of pixels at the i th gray level,

$$\mu_0 = \left(\sum_{i=0}^t \frac{in_i}{N} \right) / \left(\sum_{i=0}^t \frac{n_i}{N} \right) \quad \mu_1 = \left(\mu_T - \sum_{i=0}^t \frac{in_i}{N} \right) / \left(1 - \sum_{i=0}^t \frac{n_i}{N} \right) \quad (3.10)$$

μ_0 is the class mean for P_0 and μ_1 is the class mean for P_1 , μ_T is the total mean for the initial image. The cumulative limiting factor is computed as

$$\text{CLF}(\Delta) = \frac{\sigma_B^2(\Delta)}{\sigma_T^2} \text{ for } \Delta \geq 1. \quad (3.11)$$

The CLF is calculated for each progressive image and compared with the separability factor and the process of recursive thresholding is stopped when the condition given below is met.

$$\text{CLF}(\Delta) < \sqrt{\frac{\mu_T}{\sigma_T^2}} \quad (3.12)$$

Fig. 3.8 shows a flow diagram of the adaptive thresholding algorithm. After the image is processed, as shown in Fig. 3.9, it has the lumen region in view with background completely thresholded.

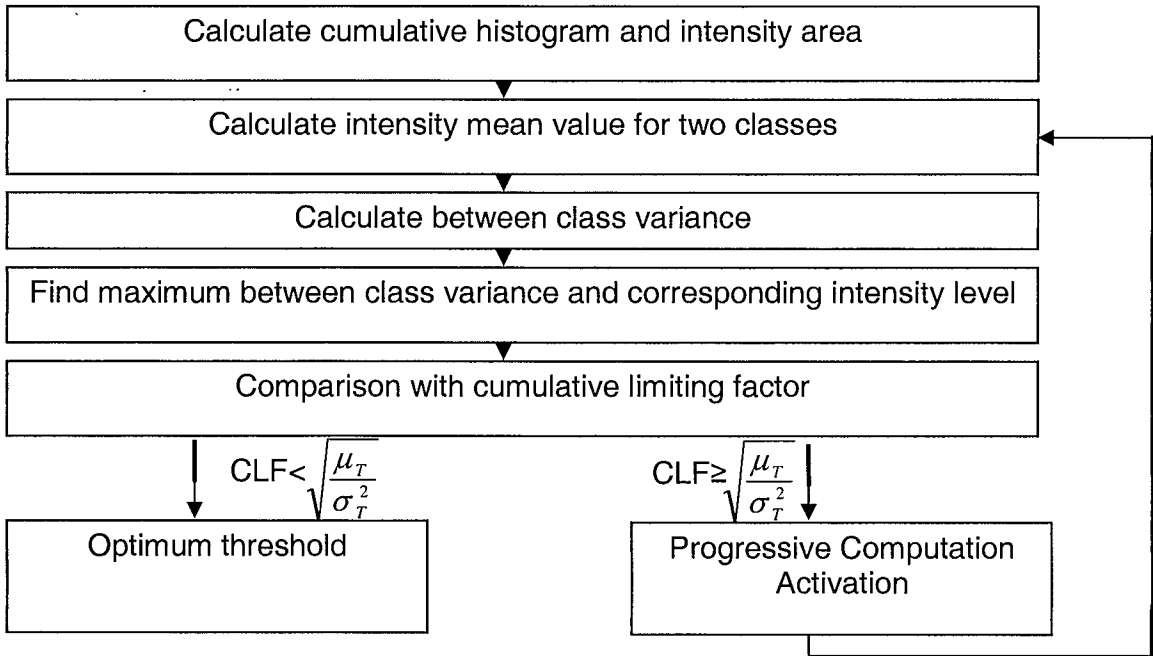


Fig. 3.8: Flow diagram of the adaptive thresholding algorithm.

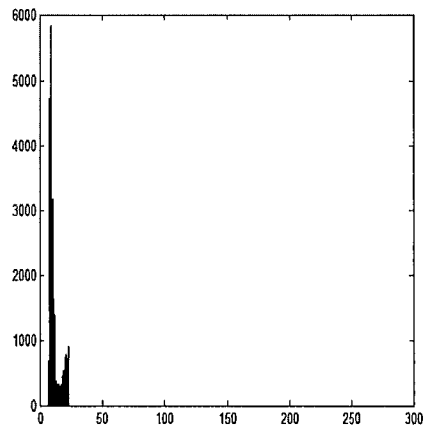


Fig. 3.9: Image thresholded with the adaptive thresholding algorithm.

The image has a spatial distribution that is random in nature. The measures of randomness [22, 23] provide a number of ways for the analysis of spatial data. It is

assumed in spatial data analysis that the observations follow a Poisson distribution. A natural test for the Poisson distribution is the ratio of the sample mean, which is called *relative variance* [24, 25]

$$V_r = \frac{\sigma_r^2}{\mu_r} \quad (3.13)$$

The frequency distribution of the object region would thus correspond to a negative binomial distribution since it has been observed that in all the experiments conducted the relative variance is greater than 1. The algorithm recursively thresholds the histogram until the maximized normalized between-class variance after the recursive iterations is lesser than the reciprocal of the square root of the relative variance of the original image. Thus, the limiting factor which incorporates the relative variance helps in stopping the algorithm at a point where the pixels in the image at this point are present as dense clusters. This clustered nature of the pixels causes only the lumen region to be left as clusters in the thresholded image.

3.1.2. Region Extraction

Precise lumen region and boundary parameters are obtained by the process of region extraction. It involves three algorithmic steps viz. pyramidal decomposition, integrated neighborhood search and back-projection.

3.1.2.1 Pyramidal quad tree structure [32]

The binarised parent image of size $M \times N$ is used to form a hierarchy of smaller images (daughter images), known as the pyramidal quad tree structure, with the top part of the

pyramid being occupied by the parent image. This pyramid is a truncated pyramid of P levels with each daughter image's height and width being reduced to half of its parent image. The pyramidal quad structure is shown in Fig. 3.10.

A count of pixels of any daughter image at the p^{th} G_p level is computed from the equation,

$$G_p = \frac{G_0}{2^{2p}} \text{ for } p = 0, 1, 2, 3 \dots, (P-1) \quad (3.14)$$

where G_0 is the parent image. Also, the intensity of the pixels $I^p(x,y)$ of the $(P-1)^{\text{th}}$ image at any given p^{th} level is given by the equation,

$$I^p(x, y) = \frac{1}{4} \sum_{i=0}^1 \sum_{j=0}^1 I^{(p-1)}(x+i, y+j) \text{ for } p = 0, 1, 2, 3 \dots, (P-1) \quad (3.15)$$

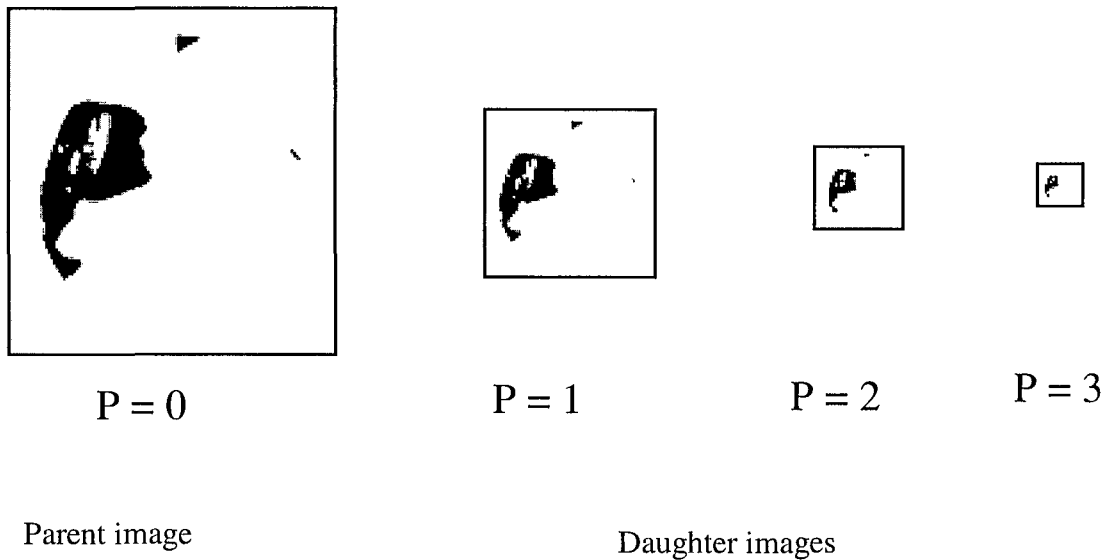


Fig. 3.10: Hierarchy of levels in a pyramidal quad tree structure.

The quasi region of interest is represented by the black pixels in the image. The center of this region qC (quasi center) in the parent image is calculated using equation 3.16.

$$x_q = \frac{1}{k} \sum_{i=1}^k x_i' \text{ and } y_q = \frac{1}{k} \sum_{i=1}^k y_i' \quad (3.16)$$

The coordinates (x_i', y_i') represent the coordinates of the i^{th} pixel in the array of black pixels present in the daughter image. The number of black pixels in the image is denoted by k . The quasi center for any particular level is computed using equation 3.17, with the upper integer value being considered.

$$(x_q^p, y_q^p) = \left[\left\lceil \frac{x_q^{p-1}}{2} \right\rceil, \left\lceil \frac{y_q^{p-1}}{2} \right\rceil \right] \quad (3.17)$$

3.1.2.2 Integrated neighborhood search [33]

This is a region analysis procedure where all the pixels in the neighborhood of the quasi center in the final daughter image are examined for similarities with their immediate neighbors. The quasi center is used as a seed to grow the lumen region. Any black or gray pixel found in the immediate neighborhood is included in the black pixel array (BA) or the gray pixel array (GA) respectively. Each of these pixels is again used for further searches in their respective neighborhoods.

This process is continued until the black and gray pixels of the region of interest are all accounted for and stored in their respective arrays. The algorithm stops searching when it encounters a white pixel. This search algorithm basically helps in finding the pixels in the region of interest.

3.1.2.3. Back projection algorithm [33]

The pixels of the daughter image stored in both the BA and GA arrays are used for back-projection. The back-projection algorithm is illustrated in Fig. 3.11.

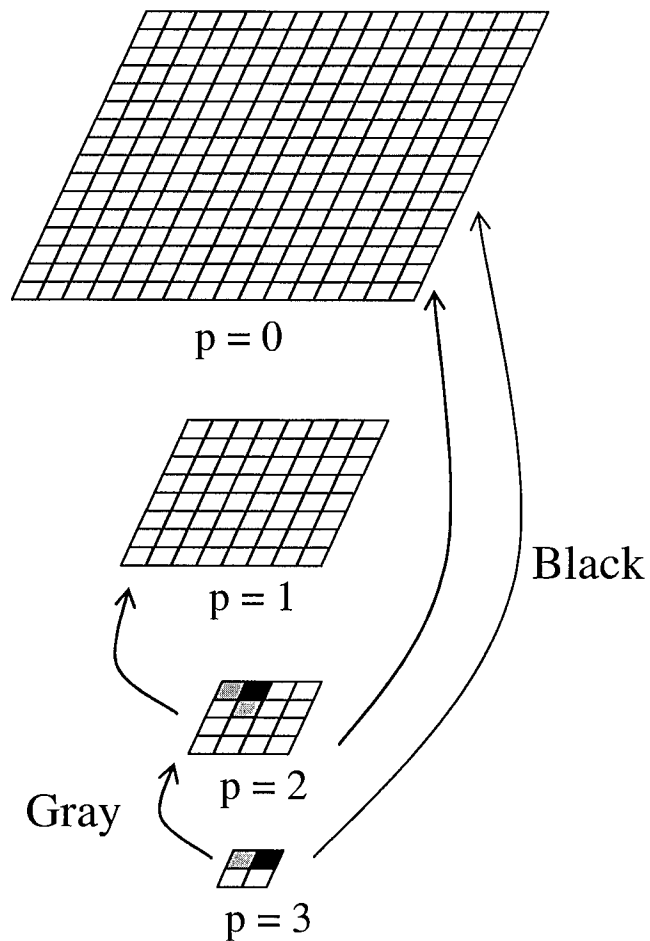


Fig. 3.11: Illustration of the back-projection algorithm.

The white pixels are all discarded. All the pixels in the BA stack are projected back onto the original parent image, with all the pixels in the original parent image corresponding to that pixel being stored in an array called the neighborhood array (NA). The pixels in the GA stack are projected back onto the immediate parent of the daughter image where four

pixels in the parent would correspond to the one GA pixel in the daughter image. In these four pixels, all black pixels are projected back onto the original parent image and the pixels corresponding to that image are again stored in NA. While the remaining pixels that are gray are projected back onto its immediate parent. This process is continued until all the pixels in the GA stack have been back-projected via their respective parent images and all the pixels in the BA stack have been back-projected onto the original image directly. The NA stack now consists of the pixels from the connected lumen region.

3.1.3. Obtaining the lumen boundary

Elimination of the higher intensity pockets, which arise in the extracted lumen region of the endoscopic images as a result of non-uniform mucosal reflections, constitutes the main aim of boundary extraction. It is performed with the help of boundary search, thinning and edge linking algorithms to get a single-pixel-width-connected boundary.

3.1.3.1. Boundary extraction [33]

The lumen region boundary is obtained with the consideration that while mapping gray pixels in a level back onto its parent image, all the white pixels in the parent image corresponding to that pixel are regarded as boundary pixels. Also, projection of black pixels from $(P-1)^{\text{th}}$ level onto the 1^{st} level involves checking for white pixels in the neighborhood. The presence of white pixels in its neighborhood calls for it to be labeled as a boundary pixel. This method gives a fair estimation of the boundary pixels and the lumen boundary.

3.1.3.2. Boundary thinning

Redundant pixels in the NA stack have to be discarded in order to get a single-pixel-width connected boundary. The reason being that the pixel boundary found from the pyramidal quad structure is of non-uniform thickness and discontinuous due to the strict rule-base followed in its two-step procedure. Boundary extraction involves a top-left and top-down preferential search, originated from the top right-most pixel in the NA stack and has the minimum y coordinate and the maximum x coordinate.

The windows in Fig. 3.12 show the sequence in which the search is conducted for a boundary pixel in the neighbors of a pixel in the NA stack. Any boundary pixel found is eliminated from the original array and then added to a new boundary pixel array to avoid repeated inclusions. This is continued until the pixel locations with the maximum y coordinate from the boundary array is searched. A second window performs a bottom-right and bottom-up preferential search in the same manner. The result of these two searches is a single-pixel-width boundary region of pixels, as shown in Fig. 3.13, enclosing the lumen region of interest.

1	8	7
2		6
3	4	5

5	4	3
6		2
7	8	1

(a) Window for top-left and top-down. (b) Window for bottom-right and bottom-up.

Fig. 3.12: Boundary extraction preferential sequence search window.



(a) With redundant pixels.

(b) Redundant pixels removed.

Fig. 3.13: Boundary thinning illustration.

3. 1. 3. 3. Boundary linking [36]

The thinned lumen boundary that is extracted has gaps in between consecutive boundary pixels. A boundary is said to be connected if it has two boundary pixels in its immediate neighborhood. In order to obtain a connected boundary, as shown in Fig. 3.14, two adjacent pixels without connectivity designated as $A(x_i, y_i)$ and $B(x_{i+1}, y_{i+1})$ are subjected to an intermediate pixel optimization scheme. The optimum locations $(x_{\text{int}}, y_{\text{int}})$ of the intermediate pixels to be added between A and B are given by,

Case I: If $|x_{i+1} - x_i| \geq |y_{i+1} - y_i|$

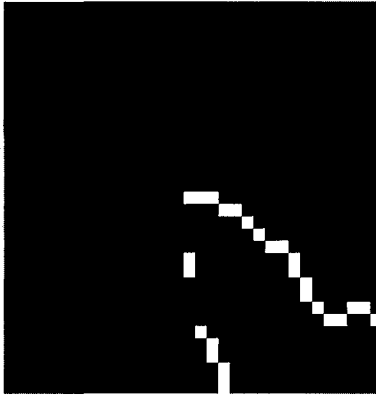
$$y_{\text{int}} = \text{int} \left(y_i + \frac{y_{i+1} - y_i}{x_{i+1} - x_i} (x_{\text{int}} - x_i) \right), \quad (3.18)$$

where x_{int} is an integer, which can possibly assume all values in the interval $[x_i, x_{i+1}]$.

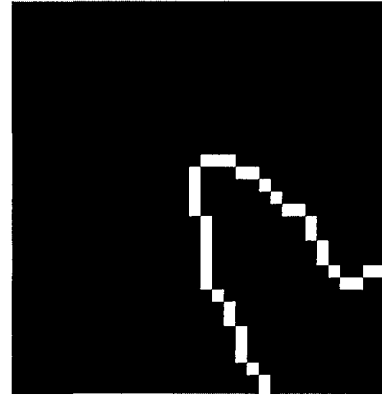
Case II: If $|x_{i+1} - x_i| < |y_{i+1} - y_i|$

$$x_{\text{int}} = \text{int} \left(x_i + \frac{x_{i+1} - x_i}{y_{i+1} - y_i} (y_{\text{int}} - y_i) \right), \quad (3.19)$$

where y_{int} is an integer, which can possibly assume all values in the interval $[y_i, y_{i+1}]$.



(a) With missing pixels.



(b) Single-pixel-width-connected boundary.

Fig. 3.14: Boundary linking illustration.

3.2 ADAPTIVE SEGMENTATION IN FACE DETECTION

Human beings vary in age, sex, and race. The color difference in human beings is a result of different amounts of melanin present in the skin. Detection of the presence of human beings in an image is a difficult task. Also, lighting conditions under which an image has been captured causes skin colors of humans to appear differently.

Pre-set thresholds for segmenting the human face in an image have failed to adapt for a diverse set of test images. This section addresses the need for an adaptive face segmentation algorithm with fairly accurate results. A novel histogram based threshold selection technique has been proposed to facilitate real-time extraction and detection of the human face. The method is based on the spatial analysis of face image data for extraction of the clustered skin regions from uniform or random-natured background. The proposed algorithm also uses wavelet and shape analysis as post-processing operations for face detection.

3. 2. 1 Histogram-based thresholding techniques

Skin thresholding is performed using the r-g histogram technique. A noted thresholding technique for skin detection is conceptualized with spatial statistics for effective skin extraction in a novel manner.

3. 2. 1. 1 Waibel et.al's Method

The chromatic colors in an image can be plotted as a three-dimensional histogram called the r-g histogram. The method is based on its argument on two very important factors in [40] which state that (1) human skin colors are present as clusters in image color space, and (2) the skin-color distribution in the normalized color space is supposed to be characterized by the multivariate normal distribution. The method also relies on cropping skin regions from images with different skin colors and then computing the r-g histogram.

The Fig. 3.15 shows the image used for the training phase of Waibel *et.al.*'s method [40]. Universal thresholds for normalized red and green colors are computed using the histogram. The gray level thresholds found from the histogram of the training image are $0.31 \leq r \leq 0.54$ and $0.23 \leq g \leq 0.39$. The image in Fig. 3.16 provides a good result with the pre-set thresholds, whereas the image in Fig. 3.17 is not properly segmented.

The use of the same set of threshold values for images with varying lighting conditions lead to many unwanted regions propping up in the thresholded image. The segmented image also had some skin regions missing. The method is not appropriate for different test images.

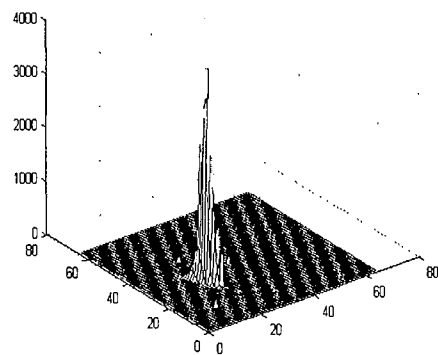


Fig. 3.15: A training image and its r-g histogram.



Fig. 3.16: Conventional skin segmentation with universal thresholds on sample image I.



Fig. 3.17: Conventional skin segmentation with universal thresholds on sample image II.

3. 2. 1. 2 Adaptive skin thresholding technique

The histogram technique proposed here automatically adapts itself to the lighting conditions and different skin colors of the human race. The image that is grabbed by the frame grabber is stored as pixel matrices containing the three digital values for each pixel with each primary color red, green and blue having a range of $\left\{0, \frac{1}{255}, \frac{2}{255}, \frac{3}{255}, \dots, 1\right\}$.

Each pixel has a definite combination defined as $Q=\{R, G, B\}$. Pixels having the same color might have different combinations of R, G and B depending on the brightness. Since it is found that brightness is irrelevant for skin color specification, chromatic data is defined as data with normalized brightness. The sum of the r, g, and b- values is thus a constant [39].

The chromatic data, which have a dependency on brightness, can be neglected, and are defined as a mapping from three-coordinate onto two-coordinate space [41].

$$f : R^3 \rightarrow R^2 \quad (3.20)$$

$$q = (r, g) = f(R, G, B) \quad (3.21)$$

and also the normalized values of the primary colors are given by equation (3.20) with the value of blue b, being redundant since $r + g + b = 1$.

$$r = \frac{R}{R + G + B} \quad \text{and} \quad g = \frac{G}{R + G + B} \quad (3.22)$$

The proposed skin segmentation method finds the thresholds for every image adaptively. The r and g values are quantized into 64 levels instead of the usual 256 levels. The image is then divided into 64 different 32×32 regions. A histogram of values with frequency of the occurrence of the combinations of red and green intensities at different pixel locations throughout the original image for each of the 64 regions is plotted. The information of the image is now stored within 4096 histogram locations of each of the 32×32 regions.

After the r-g histograms have been computed, the algorithm computes the mean and variance along the red and green axis for each region. The relative variance is calculated for each of the axis as the variance/mean ratio. The square root of this ratio is calculated and stored as DR for red and DG for green. The combination of gray levels with the relative variance ratios, $0.5 \leq DR \leq 1$ and $0.4 \leq DG \leq 0.9$, are considered to be skin regions. These color levels are then used for projecting back onto the original 32×32 region. The relative variance [24, 25] of some objects regions in face images are greater than 1. The frequency distributions of those object regions that correspond to a negative binomial distribution and cause these regions to appear as dense clusters. The clustered pixels are thresholded from the non-clustered background adaptively using the relative variance measure. It is evident from the skin thresholded image in Fig. 3.18, whose background is eliminated, and has only skin and regions having the same texture as skin.



Fig. 3.18: Sample image III thresholded with adaptive skin thresholding technique.

3. 2. 2. Face detection

The skin thresholded image has non-skin regions, which have to be eliminated for proper face detection. Further processing with wavelets, form factor analysis and morphological processing needs to be done in order to eliminate non-skin and non-face regions.

3. 2. 2. 1. Wavelet Analysis

Wavelet analysis provides a multi scale analysis with coefficient matrices for spatial and frequential decomposition. A texture analysis aided by wavelets, as suggested in [52], is used to remove these regions by performing wavelet packet decomposition on the r-g histogram thresholded intensity plane of the image. A set of feature vectors is extracted from the wavelet packet coefficients in each area.

Every region in the histogram thresholded image is bounded by a box and is subjected to texture analysis using wavelets. A signal $s(t)$ is represented in discrete wavelet series as,

$$c_{n,k} = \frac{1}{2^{n/2}} \int s(t) \psi^*(2^{-n}t - k) dt \quad (3.23)$$

where, $\psi(t)$ is the mother wavelet which ensures a non-redundant and comprehensive representation of the original signal. A dyadic scale factor (scales and positions based on powers of 2) with scale level n and localization parameter k is used. A successive decomposition of the continuous signal by a pair of low pass $[h(\cdot)]$ and high-pass $[g(\cdot)]$ filters gives the discrete wavelet transform. At coarser resolutions the low pass filter provides the approximation of the signal, and the high-pass filter provides the details of the signal. Two-dimensional signals such as images are wavelet transformed into the discrete domain by applying the two filters along each axis to get the *approximation* image with the low pass filter, and *detail* images with the high-pass filter.

An n-level wavelet decomposition results in the signal being represented as:

$$A_n = [h_x * [h_y * A_{n-1}]_{\downarrow 2,1}]_{1,2}$$

$$D_{n1} = [h_x * [g_y * A_{n-1}]_{\downarrow 2,1}]_{1,2}$$

$$D_{n2} = [g_x * [h_y * A_{n-1}]_{\downarrow 2,1}]_{1,2}$$

$$D_{n3} = [g_x * [g_y * A_{n-1}]_{\downarrow 2,1}]_{\downarrow 1,2} \quad (3.24)$$

The image is first split into an approximation image and its details. An approximation image is further subject to decomposition into a second-level of approximation and details images. $A *$ denotes the convolution product, $A_0 = I(x,y)$ denotes the original image and $\downarrow 2,1$ (1, 2) signifies sub sampling along rows and columns. Fig. 3.19 shows the wavelet decomposition at three levels.

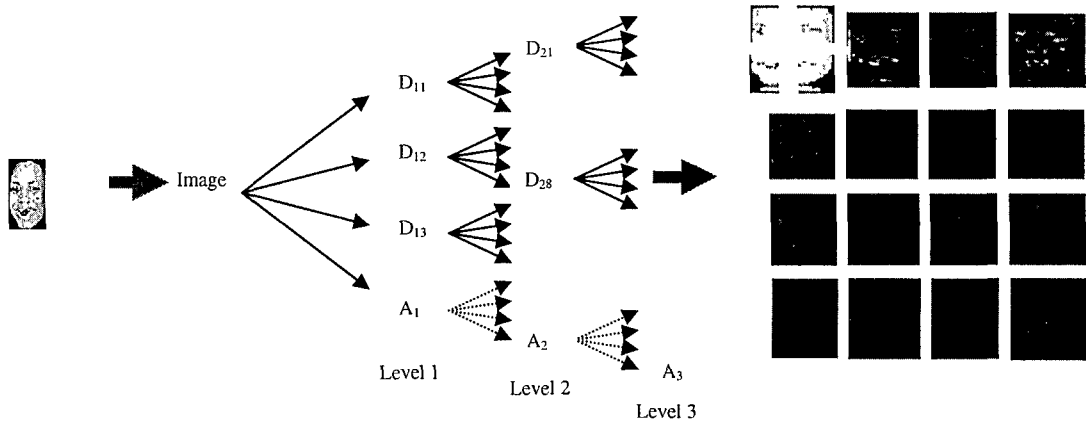


Fig. 3.19: Wavelet decomposition into detail and approximation images shown at 3 levels.

The original image is thus represented as a set of sub-images $\{ A_n, D_{ni} \}$ where A_n is the approximation image at level n obtained by low-pass filtering and D_{ni} ($i = 1, 2, 3$, for vertical, horizontal and diagonal directions respectively) denotes details images obtained by band-pass filtering in a given direction.

The choice of coefficients for the $h(\cdot)$ and $g(\cdot)$ filters are from the experimental results of [50, 51] with their Z-transforms given by the equations:

$$H(z) = 0.853 + 0.3777(z + z^{-1}) - 0.111(z^2 + z^{-2}) - 0.024(z^3 + z^{-3}) + 0.038(z^4 + z^{-4}) \quad (3.25)$$

$$G(z) = -z^{-1}H(-z^{-1}). \quad (3.26)$$

The filters considered are orthogonal and follow the equation:

$$\sum_n h(n-2k)g(n-2l) = 0, \forall (k, l), \quad (3.27)$$

with the low-pass filter being symmetric.

The approximation image is further decomposed into four sub-images and the standard deviation for the four sub-images (σ_i , $i=0, 1, 2, 3$) and the standard deviation for the 15 detail images (σ_i , $i=4, 5, 6, 7 \dots 19$) are all calculated. It has been assumed by the authors that the approximation images are distributed according to the Gaussian law, whereas the detail images are supposed to be distributed according to the Laplacian law. The mean value differences of the approximation image are not considered so as to let the distance measure be independent of the lighting conditions. The mean values of the detail images are set to zero because of the design of the filters. The distance measure as suggested in [56] is calculated by the equation:

$$D(v_k, v_l) = \frac{1}{2} \sum_{i=0}^3 \ln \left(\frac{\sigma_{ik}^2 + \sigma_{il}^2}{2\sigma_{ik}\sigma_{il}} \right) + \sum_{i=4}^{15} \ln \left(\frac{\sigma_{ik} + \sigma_{il}}{2\sqrt{\sigma_{ik}\sigma_{il}}} \right) \quad (3.28)$$

where $D(v_k, v_l)$ is the distance measure between two feature vectors denoted by v_k which is the feature vector of the original image and v_l is the feature vector of the prototype vector which has been computed using a set of images. A given region is classified as skin if $D(v_k, v_l) < 7.0$, else it is rejected. Fig. 3.20 shows the result of wavelet analysis.

3. 2. 2. 2. Form factor analysis

The resultant skin regions are subjected to shape analysis by first computing the form factor for each candidate region. Form factor is given by the equation:

$$ff = (4\Pi * Area) / (Perimeter^2). \quad (3.29)$$

This is primarily to weed out any skin regions, which are other than the face regions. Every candidate region, whose shape is not close to being circular and form factor is less than 0.7 if discarded. All the remaining regions are either faces or very-circular skin regions as shown in Fig. 3.21.

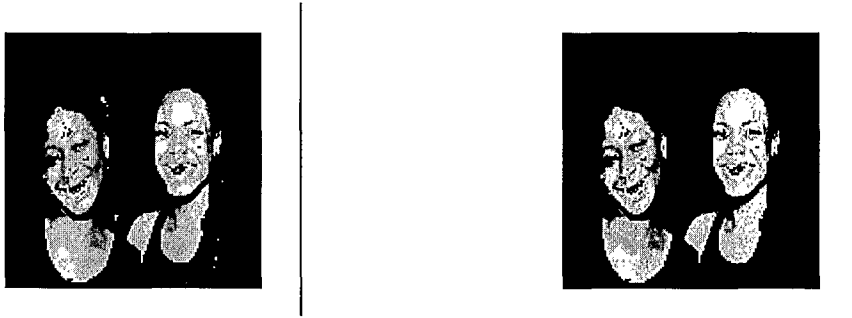


Fig. 3.20: Sample Image III after wavelet analysis.

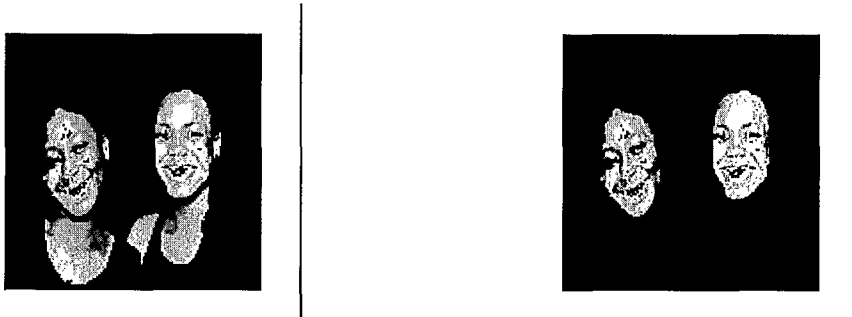


Fig. 3.21: Sample Image III after form factor analysis.

3. 2. 2. 4. Morphological operation

The boundaries of the candidate face regions are back-projected onto the original image to obtain regions which are supposed to be faces. The resulting image is then thresholded

using the automated thresholding algorithm (ATA) as a gray-level image. This helps in finding all regions with dark spaces and cavities in them. The result of this operation is shown in Fig. 3.22.

A structural element comprising of a 1×3 matrix of ones erodes and widens these dark features like eyes, nose and eyebrows in the face regions and gives the output as shown in Fig. 3.23.

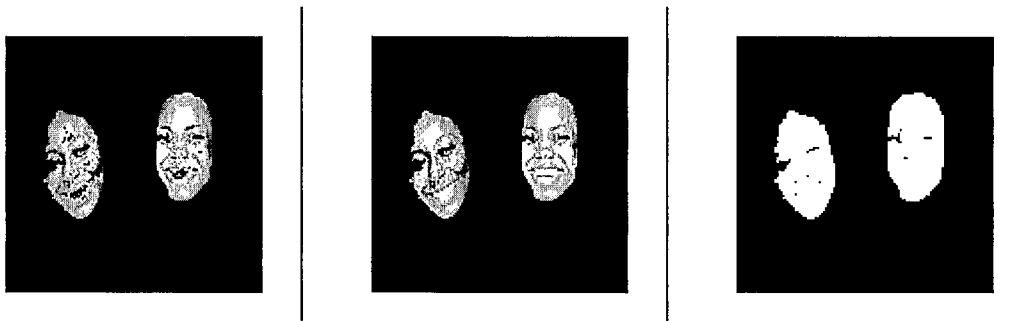


Fig. 3.22: Candidate face regions back-projected and thresholded using the ATA technique.

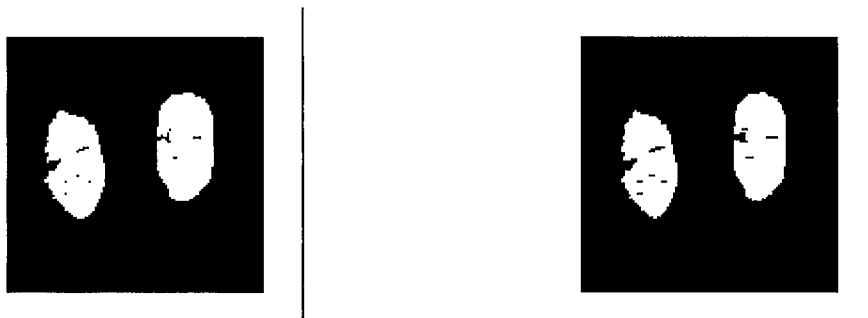


Fig. 3.23: Morphological operation on the ATA thresholded candidate face regions.

Now if the program finds the required number of holes (2 for a face) in the candidate face region it calls it a face and bounds it with a box. The choice of the required number of holes is supposed to be 2 to include profile images where the probable holes in the candidate face region would be a maximum of 2.

3. 3. Summary

A novel adaptive thresholding technique for faster and accurate lumen region extraction has been presented. The method incorporates a dispersion factor for computation of the factor of separability in thresholding the endoscope image. It is more accurate and faster than the adaptive progressive thresholding algorithm. Furthermore, an accurate skin extraction technique with a novel adaptive thresholding method is also presented. Spatial analysis has proved that the negative binomial distribution characteristics can be used to validate both the proposed algorithms for their success in selecting the right threshold adaptively. When compared to the traditional methods of threshold selection, the proposed method outperformed existing techniques by improving on their accuracy and ease of use. Wavelets and shape analysis aided texture segmentation and face region identification. Realization of the proposed techniques with optimized hardware would increase the speed of the methods appreciably.

CHAPTER 4

SIMULATION RESULTS

The adaptive segmentation algorithms were developed on an Intel Pentium IV computer with a processor speed of 2.0 GHz and 256MB RAM. Experiments were conducted on sample images with complex object regions in the Windows NT environment using Matlab software's version 6.0, release 12. Simulation results are presented in this chapter.

4.1. Lumen Region Extraction with Adaptive Thresholding Algorithm

Endoscopic imaging is a field in which thresholding is a difficult task due to the unpredictable image environment. The intestinal tract is peculiar because its reflective characteristics vary from person to person due to age and different eating habits. It is , therefore, entirely unpredictable and this makes it difficult to pre-determine the threshold points. The threshold is aptly determined when the characteristics of the image are considered.

Fig. 4.1 shows a 256×256 endoscopic image. The objective of thresholding in this image is to extract the hollow space boundaries so as to enable an endoscope to pass through the tract. The thresholded result indicates that the hollow space has been effectively extracted from the image although the thresholded image has other clusters. The largest cluster corresponds to the lumen region of the intestinal tract. The quasi center coordinates of the lumen region for this image was found to be (130, 86). Extracting the lumen boundary from the thresholded image involves searching the neighborhood of the quasi center. Faster computation to eliminate ambiguous regions

from the thresholded image is facilitated by using pyramidal quad tree structure described in chapter 3 section. 1. 2. 1.

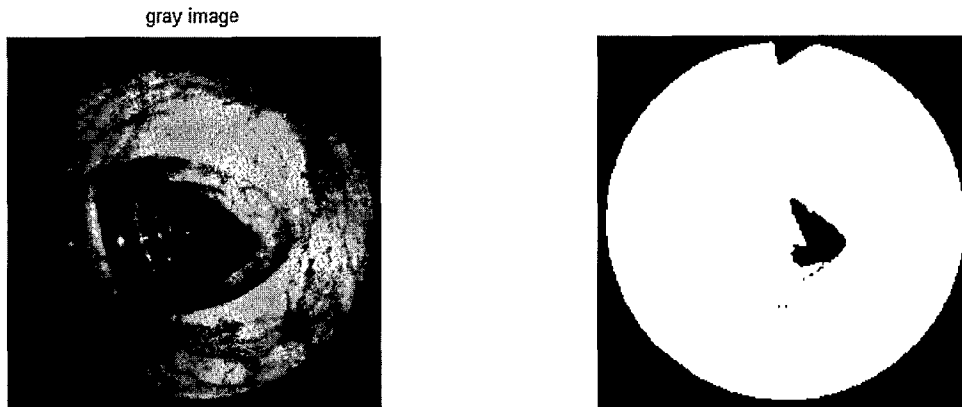


Fig. 4.1: Endoscopic image thresholded using ATA.

A four tier structure is generated from the binarised parent image. The 3 daughter images generated from the process can be seen in Fig. 4.2. Image compression causes the resolution of the image to decrease for the daughter images.

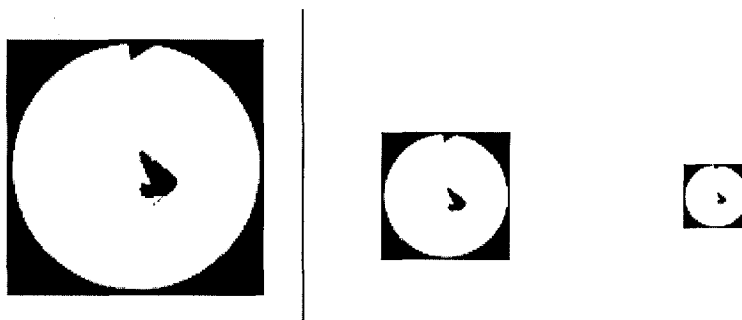


Fig. 4.2: Daughter images generated using the quad structures

The integrated neighborhood search algorithm eliminates the ambiguous regions in the image as is evident from the result in Fig. 4.3. The region found from the integrated neighborhood search routine is used to back-project and obtain the lumen region of the endoscopic image. The lumen region after back projection is shown in Fig. 4.4.



Fig. 4.3: Integrated neighborhood search result for the daughter image.



Fig. 4.4: Back-projection from a daughter image onto the parent image.

The boundary of the lumen region found in Fig. 4.4 is obtained by the boundary extraction process described in chapter 3 section 1. 3. 1 and is shown in Fig. 4.5. This boundary has redundant pixels in it. The thinning algorithm effectively eliminates these redundant pixels to obtain a single-pixel-width boundary as shown in Fig. 4.6. A single-

pixel-width-connected boundary is the final result shown in Fig. 4.7, which has the lumen boundary highlighted in the backdrop of the original image.



Fig. 4.5: Edge-detected parent image.



Fig. 4.6: Thinning algorithm application and binarization.

Additional gastrointestinal images and their extracted boundaries are shown in Figs. 4.8 and 4.9. Both the images are of size 256×256 and were captured by an endoscope. Results are quite conclusive and show accurate boundaries that are needed by the micro robot to navigate through the intestinal tract.



Fig. 4.7: Thinning result of sample image with final boundary extracted.



Fig. 4.8: Original sample image II with extracted lumen boundary.



Fig. 4.9: Original sample image III with extracted lumen boundary.

Table 1 provides the difference in processing times for three test images between the APT-based method and the proposed ATA-based method. The percentage decrease in processing times is also shown in the table. An overall computation time reduction of 35.82% is achieved by ATA. It can be seen that there is a substantial increase in the speed and accuracy of the process that facilitates online feature extraction and analysis.

Table 1. Experimental results showing difference in processing time
between APT and ATA based methods.

Test image	Processing time in seconds		Overall reduction in processing time	
	APT-based	ATA-based	In seconds	Percentage improvement in speed
Sample Image 1 (256 × 256)	2.2780	1.4604	0.8176	35.89%
Sample Image 2 (237 × 245)	2.9370	1.9273	1.0097	34.38%
Sample Image 3 (256 × 256)	2.1960	1.3793	0.8167	37.19%

4. 2. Adaptive Segmentation for Face Detection

The image shown in Fig. 4.10 is the subject for the proposed face detection routine. The histogram technique, coupled with the relative variance, is used to extract the skin regions from the image. The results of the skin extraction are shown in Fig. 4.11. This image has skin regions as well as non-skin regions. These regions emerge due to the objects in the image which have the same color content as the skin regions. The non-skin regions in the thresholded image are removed by using the wavelet analysis. The result of the wavelet analysis in Fig. 4.12 shows the skin regions only, properly segmented from the background.



Fig. 4.10: Sample image I for face detection routine.



Fig. 4.11: Result of adaptive skin threshold method.

This image now has regions which are ears, neck and limbs in a human image which are unwanted regions in our segmentation task. Shape analysis described in chapter 3 Sections 2.2.2 and 2.2.3 extracts the face regions from Fig. 4.12 using the basic property of a face being nearly circular or elliptical in shape. Fig. 4.13 shows this result with all the unwanted regions in the image segmented out.

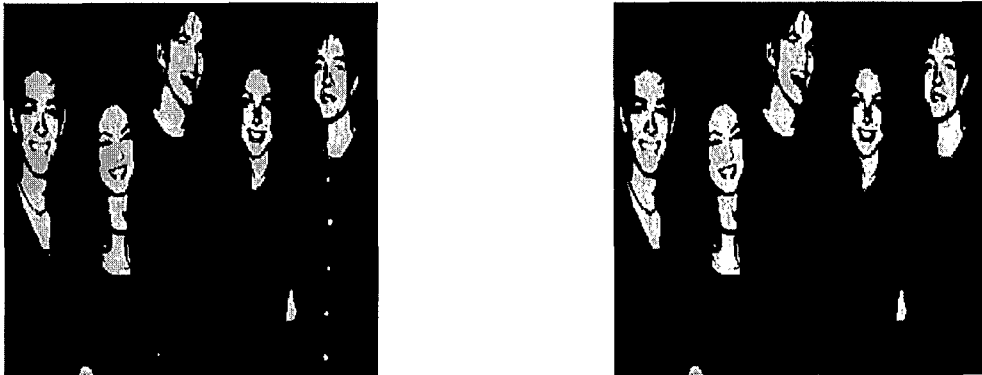


Fig. 4.12: Result of the wavelet analysis result of the grayscale image.

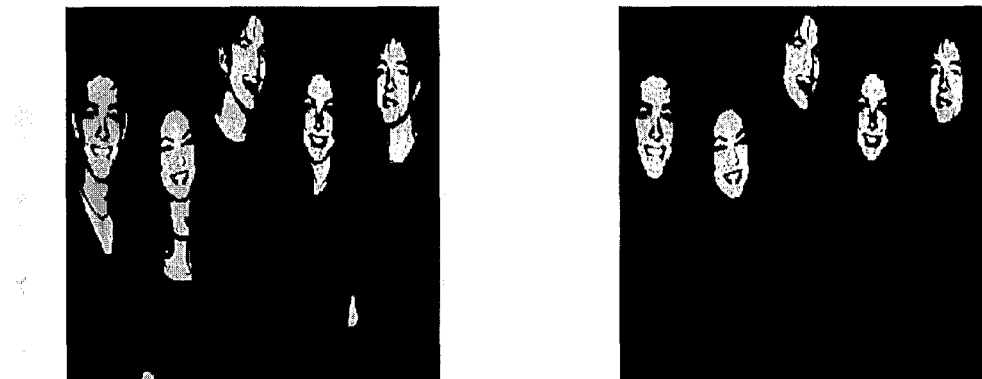


Fig. 4.13: Result of shape analysis using the form factor.

An application of the adaptive thresholding algorithm, from the endoscopic lumen extraction process, over Fig. 4.13 gives a binarised image, which has the face regions as objects with holes. Fig. 4.14 is the result of this process. The number of holes is counted for each candidate region. If they satisfy the number required to be classified as a face region, the region is identified as a face as shown in Fig. 4.15.

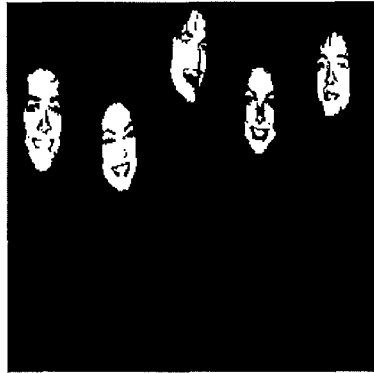


Fig. 4.14: Binarized version of image in Fig. 4.13.



Fig. 4.15: Sample image I and the final result showing faces bound with a box.

All the images shown in Fig. 4.16, Fig. 4.17 and Fig. 4.18 are of size 256×256 . The choice of the image size was 256×256 to facilitate wavelet processing which require image dimensions to be of the order of 2^n , where $n = 2, 3, 4, \dots$



Fig. 4. 16: Sample image II and its final result .

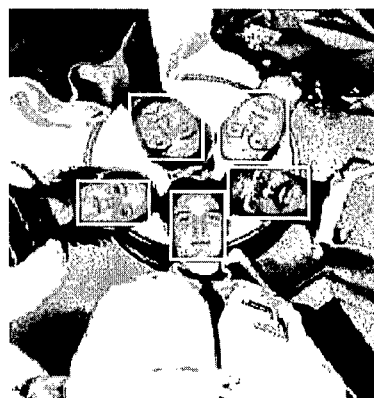


Fig. 4.17: Sample image III and its final result.



Fig. 4.18: Sample image III and final result; also shows two of the missed detections.

Table 2 presents results of the comparison of the conventional face detection algorithm to the proposed algorithm by testing a set of 20 images with 75 human faces. An increase of 9% in accuracy has been observed for objects that are clearly visible but are similar to each other in color content.

Table 2. Comparison of the conventional r-g histogram thresholding algorithm with the proposed face detection method.

Result of face detection	Conventional r-g histogram thresholding algorithm		Relative variance-based r-g histogram thresholding algorithm	
	Cases	Percentage Accuracy	Cases	Percentage accuracy
Face detected	63	84%	70	93%
Face missed	12	16%	5	6%

4. 3. Summary

An adaptive segmentation algorithm for lumen region extraction has been simulated and results were illustrated in this section. It has been observed that the lumen region extraction technique achieved a 36% improvement in computational time when compared with the conventional extraction method. Also, the method has been found to be accurate in region and boundary extraction from images with complex background environment. An adaptive skin extraction technique for human face detection based on spatial analysis has also been simulated and tested. The proposed method is 9 % more accurate than the conventional skin extraction technique. The adaptive algorithm performs well with images in varying and poorly lit conditions.

CHAPTER 5

CONCLUSION

This thesis has mainly focused on the development of adaptive image segmentation techniques for endoscopic lumen extraction and human face detection from images with complex lighting environment. The manual identification of these borders is time-consuming, tedious and prone to error. A novel histogram-based adaptive thresholding procedure for lumen region extraction incorporating spatial analysis of image data has been presented in this thesis. The task of identifying the lumen boundary in complex lighting environment is a challenging problem to which the application of automated thresholding algorithm provides a promising solution.

A novel thinning algorithm has also been presented to aid the region boundary processing. The characteristics of the proposed system and its performance have been tested on a standard platform. Experimental evaluation showed that the ATA-based technique is robust and superior enough to conventional techniques of threshold selection for the extraction of lumen region in endoscopic images. It differs from the methods presented in the literature because of its accuracy to extract boundaries, low computational complexity and the ease with which it can be optimized and parallelized. Results have shown a 36 % decrease in computation time facilitating high-speed response for real-time endoscopic applications.

Secondly, the ability to identify human faces in images with varying lighting environments is needed for face detection applications. A novel adaptive skin thresholding algorithm for face detection without pre-trained universal thresholds has also been presented. Analyses show that this relative variance based method extracts skin

very effectively when compared to existing techniques. Anomalies that arise due to training of images in conventional techniques have been addressed and an accuracy improvement of 9% has been noted for a diverse set of imagery in adverse lighting conditions that have been tested to validate the system's performance. High-speed hardware and software optimization could be used to achieve faster processing time for video frame rates. Work is in progress to adapt the system to pose and motion invariance, and segment static color images using dispersion factor based lighting compensation methods.

REFERENCES

1. Pal, N. R., and S.K. Pal., "A review on image segmentation techniques," *Pattern Recognition*, vol.26, no. 9, pp: 1277-94. 1993.
2. K. S. Fu, "A survey on image segmentation", *Pattern Recognition*, vol. 13, pp. 3-16, 1981.
3. R. M. Haralick, and L. G. Shapiro, "Survey: Image Segmentation techniques", *Comput. Vision Graphics Image Proc.*, vol. 29, 1985, pp. 100-132, 1985.
4. J. Chen and T. N. Pappas, "Adaptive image segmentation based on color and texture," in *Proc. ICIP-02*, vol. 3, (Rochester, NY), pp. 777--780, Sept. 2002.
5. A. Laine and J. Fan, "An adaptive approach for texture segmentation by multi channel wavelet frames," *Technical Report TR-93-025*, Center for Computer Vision and Visualization, Univ. of Florida, Gainesville, FL, Aug. 1993.
6. L. Tian, D. C. Slaughter, and R. F. Norris, "Outdoor field machine vision identification of tomato seedlings for automated weed control," *Transactions of the ASAE*, vol. 40, no. 6, pp: 1761-1768, 1997.
7. M. Droske, and B. Meyer, and M. Rumpf, and C. Schaller, "An adaptive level set method for medical image segmentation," in *Proc. of the Annual Symposium on Information Processing in Medical Imaging*, R. Leahy and M. Insana (ed), Springer, Lecture Notes Computer Science, 2001.
8. Kumar S., Kassim, I. M., and Asari, V.K., "Design of a Vision-guided Microrobotic Colonoscopy", *Advanced Robotics*, vol. 14, no. 2, pp. 87-104, 2000.
9. P. Dario, M.C. Carrozza, L. Lencioni, B. Magnani, S. D'Attanasio, "A Micro Robotic System for Colonoscopy", *Proc. of the International Conference on Robotics and Automation (ICRA '97)*, Albuquerque NM, pp. 1567-1572, April 20-25, 1997.
10. B. Kim, Y. Jeong, H. Lim, T. S. Kim, J. Park, P. Dario, A. Menciassi and H. Choi, "Smart Colonoscope System," *IEEE/RSJ International Conference on Intelligent Robots and Systems, Switzerland*, Sep 30-Oct 4, 2002.

11. R. Chellappa, C.L. Wilson, and S. Sirohey., "Human and machine recognition of faces: A survey," *Proc. IEEE*, vol. 83, pp. 705–740, May 1995.
12. R.-L. Hsu, Mohamed Abdel-Mottaleb and A. K. Jain, "Face Detection in Color Images", *IEEE Transactions on PAMI*, vol. 24, no.5, pp. 696-706, May 2002.
13. V. Wu, R. Manmatha, and E. M. Riseman, "Finding text in images", *Proc. ACM Int. Conf. Digital Libraries*, 1997.
14. V. Wu and R. Manmatha, "Document image clean-up and binarization", *Proc. SPIE Symposium on Electronic Imaging*, 1998.
15. Margaret M. Fleck, David A. Forsyth, and Chris Bregler, "Finding naked people," *European Conference on Computer Vision*, vol. 2, pp. 593–602. Springer-Verlag, 1996.
16. Sahoo, P. K., S. Soltani and A. K. C. Wang., "A survey of thresholding techniques," *Computer Vision, Graphics, and Image Processing*, vol. 41, pp. 233-60, 1988.
17. Lee, S. U., S. Y. Chung, and R. H. Park., "A comparative performance study of several global thresholding techniques for segmentation," *Computer Vision, Graphics, and Image Processing*, vol. 52, pp. 171-190, 1990.
18. J. S. Weszka, "A survey of threshold selection techniques," *Comput. Graphics Image Proc.*, Vol. 7, pp. 259-265, 1978.
19. Otsu, N., "A thresholding selection method from gray-level histogram,". *IEEE Transactions on Systems, Man, and Cybernetics*, vol. 9, no. 1, pp. 62-66, 1979.
20. Cheriet M., Said J.N. and Suen C.Y., "A Recursive Thresholding Technique for Image Segmentation, " *IEEE Trans. on Image Processing*, vol. 7, no. 6, pp. 918-922, June 1998.
21. Asari K. V., Srikanthan T., Kumar S., and Radhakrishnan D., "A Pipelined Architecture for Image Segmentation by Adaptive Progressive Thresholding," *Journal of Microprocessors and Microsystems*, vol. 23, pp. 493-499, 1999.

22. G.J.G. Upton and B. Fingleton, "Spatial Data Analysis by Example, Volume 1, Point Pattern and Quantitative data" *Wiley*, 1985.
23. A. Rogers, "Statistical Analysis of spatial dispersion the quadrat method," *Methuen Inc.*, 1974.
24. A. R. Clapham, " Over dispersion in grassland communities and the use of statistical methods in plant ecology," *Journal of Ecology*, vol. 24, pp. 232-251, 1936.
25. P. L. Rosin, "Thresholding for change detection", *Proc. of International Conference of Computer Vision (ICCV-98)*, pp. 274–279, 1998.
26. Deepthi P. Valaparla and Vijayan K. Asari , "An adaptive technique for the extraction of object region and boundary from images with complex environment," *IEEE Computer Society Proceedings of 30th International Workshop on Applied Imagery and Pattern Recognition, AIPR - 2001* , Washington DC, USA, pp. 194 - 199, October 10 - 12, 2001.
27. D. Ziou, S. Tabbone, "Edge Detection Techniques- An Overview," *technical report, No. 195*, Dept Math & Informatique. Université de Sherbrooke, 1997.
28. K. V. Asari, S. Kumar, and D. Radhakrishnan, "Technique of Distortion Correction in Endoscopic Images using a Polynomial Expansion," *IEE Journal of Medical & Biological Engineering & Computing* , vol. 37, no. 1, pp. 8-12, January 1999.
29. K. V. Asari, S. Kumar, and D. Radhakrishnan, "A New Approach for Nonlinear Distortion Correction in Endoscopic Images based on Least Squares Estimation," *IEEE Transactions on Medical Imaging* , vol. 18, no. 4, pp. 345-354, April 1999.
30. J. Weng, A. Singh, and M. Y. Chiu, " Learning-based ventricle detection from cardiac MR and CT images," *IEEE Trans . Med. Imag.*, vol. 10, pp 578-591, 1997.
31. R. Ohlander, K. Price, D.R. Reddy, "Picture segmentation using a recursive region splitting method," *Comput. Graphics Image Process.*, vol. 8, pp. 313-333, 1978.

32. Gul N. Khan and D. F. Gillies, "Parallel-Hierarchical Image Partitioning and Region Extraction", *Computer Vision and Image Processing*, (Eds. L. Shapiro and A. Rosenfeld) pp. 123-140, Academic Press, 1992.
33. K. V. Asari, S. Kumar, and D. Radhakrishnan, "Technique of Distortion Correction in Endoscopic Images using a Polynomial Expansion," *IEE Journal of Medical & Biological Engineering & Computing* , vol. 37, no. 1, pp. 8-12, January 1999.
34. J. P. Gambotto, "A new approach to combining region growing and edge detection", *Pattern Recognition Letters*, vol. 14, pp. 869-875, 1993.
35. M. Ahmed, and R. K. Ward, "Fast one-pass knowledge-based system for thinning," *J. Electron. Eng.*, vol. 7, no. 1, pp. 111-116, 1998.
36. R. Ohlander, K. Price, D.R. Reddy, "Picture segmentation using a recursive region splitting method," *Comput. Graphics Image Process*, vol. 8, pp. 313-333, 1978.
37. M. J. Swain and D. H. Ballard, "Color indexing," *International Journal of Computer Vision*, vol. 7, no. 1, pp. 11-32, November 1991.
38. Y. Rubner, C. Tomasi, and L.J. Guibas, "A metric for distributions with applications to image databases," *In Proceedings of the 6th International Conference on Computer Vision (ICCV)* IEEE Computer Society Press., pp 59-66, Bombay, January 1998.
39. G. Wyszecki and W.S. Stiles, "Color Science," *Wiley, New York*, 1982.
40. J. Yang , W. Lu and A. Waibel, " Skin color modeling and adaptation," *Proceedings Third Asian Conference on Computer Vision*, vol. 2, pp. 142-147, 1998.
41. H. M. Hunke., "Locating and tracking of human faces with neural networks," *Technical Report CMU-CS-94-155*, Carnegie Mellon University, 1994.

42. M. Hunke and A. Waibel., "Face locating and tracking for human-computer interaction," *Proceedings of 28th Asilomar Conference on Signals, Systems and Computers* at Monterey, California Pittsburgh. School of Computer Science, Carnegie Mellon University, 1994.
43. B. Schiele and A. Waibel., "Gaze tracking based on face color," *International Workshop on Automatic Face and Gesture Recognition*, 1995.
44. T.C. Chang, T.S. Huang, and C. Novak, "Facial feaure extraction from color images," *Proc. the 12th IAPR International Conference on Pattern Recognition*, vol. 2, pp. 39-43, 1994.
45. J. Yang and A. Waibel, "A real-time face tracker," *Proceedings of the Third IEEE Workshop on Applications of Computer Vision (Sarasota, Florida, 1996)*, pp. 142- 147 ("Tracking human faces in real-time," Technical Report CMU-CS-95-210, CS department, CMU), 1995.
46. A. R. Clapham, " Over dispesion in grassland communities and the use of statistical methods in plant ecology," *Journal of Ecology*, vol. 24, pp. 232-251, 1936.
47. P. L. Rosin, "Thresholding for change detection", *Proc. of International Conference of Computer Vision (ICCV-98)*, pp. 274–279, 1998.
48. I. Daubechies, "The wavelet transform, time-frequency localization and signal analysis," *IEEE Trans. Inform. Theory*, vol. 36, pp. 961–1005, 1990.
49. S. Mallat, "A theory of multi-resolution signal decomposition: The wavelet representation," *IEEE Trans. Pattern Anal. Machine Intell.*, vol. 11, pp. 674–693, 1989.
50. M. Smith and T. Barnwell, "Exact reconstruction techniques for tree structured subband coders," *IEEE Trans. Acoust., Speech, Signal Processing*, vol. ASSP-34, pp. 434–441, Mar. 1986.
51. P. H. Westerink, J. Biemond, and D. E. Boekee, "Subband coding of color images," *Subband Image Coding*, J. W. Woods, Ed. Boston, MA: Kluwer, pp. 193–228, 1991.

52. Garcia C., Zikos G., Tziritas G., "Wavelet Packet Analysis for Face Recognition", *Image and Vision Computing*, vol.18, no. 4, pp.289-297, February 2000.
53. Y. Fu, "Handbook of Pattern Recognition and Image Processing," New York: Academic, 1986.
54. T. Kailath, "The divergence and Bhattacharyya distance measures in signal selection," *IEEE Trans. Commun.*, vol. com-15, pp. 52–60, 1967.
55. D. Kazakos, "The Bhattacharyya distance and detection between Markov chains," *IEEE Trans. Inform. Theory*, vol. it-24, pp. 747–754, June 1978.
56. A. Eleftheradis and A. Jacquin, "Model-assisted coding of video teleconferencing sequences at low bit rates," in *Proc. IEEE Int. Symp. Circuits and Systems*, pp. 3.177–3.180, 1994.

CURRICULUM VITAE

Deepthi P Valaparla

931 Rockbridge Ave #250,
Norfolk VA-23508

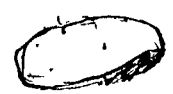
Phone: (757) 423-1239
Mobile: (757) 343-4682
Email: dvala001@odu.edu

- **Educational Background:**
 - M.S. in Electrical Engineering, May 2003, GPA: 3.5, Old Dominion University, Norfolk VA. *Focus:* Automated image segmentation of objects in complex lighting environments.
 - B.Tech. in Electronics and Communication Engineering, June 2000. GPA: 3.5, Jawaharlal Nehru Technological University Hyderabad-32, A.P India. *Focus:* Worked on computer networks and medical diagnostic equipment in funded projects
- **Interests:**
 - Object/Region detection in endoscopic images
 - Biometrics and Image Processing
 - Modular neural networks
- **Areas of Expertise**
 - Extensive experience in digital signal/image processing algorithms
 - Well-versed on computer vision:
 - Edge detection, segmentation, motion analysis, etc.
 - 3D video processing and registration
 - Familiar with programming languages/tools (MATLAB, MAXPLUS2, VHDL, C etc.) and OS platforms (Window95, Window NT, etc.)
- **Practical Experience:**
 - Assistant Researcher, 2000-Current, Old Dominion University, Norfolk VA
 - Developed a novel automated skin segmentation algorithm for face detection
 - Author of an adaptive endoscopic segmentation algorithm for lumen region extraction
 - Academic Teaching Assistant, 2001-Present, Academic Skills Center(Old Dominion University) Norfolk VA,
 - Assist students with documented learning and physical disabilities
 - Teaching Assistant, 2001-2002, Old Dominion University Norfolk VA
 - Evaluated coursework and various projects implemented by students during the course.
 - Member of the grading committee
 - Student Researcher, 1999-2000, ECIL, Hyderabad A.P India
 - Development of screening test equipment MS 5605A for AIDS virus, based on Enzyme Linked Immuno-Sorbent Assay (ELISA)
- **Publications:**
 - Deepthi P. Valaparla and Vijayan K. Asari, “ An adaptive technique for the extraction of object regions from images with complex environment”, *IEEE Computer Society Proceedings of 30th International Workshop on Applied Imagery and Pattern Recognition, AIPR-2001, Washington DC, USA*, pp. 194-199, Oct. 10 – 12, 2001.

D.C.
LAX

Electrical-
Production.

New Heavens :- 



Rent \rightarrow \$850 - (Double Bed) .

\$1000
\$(650-700) (Single Bed) .

on campus \rightarrow X off campus \rightarrow \checkmark

\$8/7/hr

(New Heavens / New York (JFK))

Prime Time
Limo.

\$65-\$70 (1 1/2 hr)

Accommodation \rightarrow (Sudheer Samson)

COURSE \rightarrow \$1600 / \$1690 ::::

4

University of
New Heavens.

(1 year - 1 sem)

Year 3 Sem.

TU 5105.888 .LSM 2005 ✓

QA 76.76 .H94 C36 2004 ✓

QA 76.76 .H94 M47 2004 ✓